Ministério da
Ciência e Tecnologia

INPE-16666-RPQ/846

RESEARCH AND DEVELOPMENT IN A SMALL SPHERICAL TOKAMAK

Gerson Otto Ludwig
Edson Del Bosco
Joaquim José Barroso
Luiz Angelo Berni
Maria Célia Ramos Andrade
Julio Guimarães Ferreira
Rogério Moraes Oliveira
Pedro José Castro
José Osvaldo Rossi
Carlos Shinya Shibata
Ramesh Nayaranan
Raul Murete Castro

Original document registry:
<http://urlib.net/sid.inpe.br/mtc-m19@80/2010/02.12.16.37>

INPE
São José dos Campos
2010

PUBLISHED BY:

Instituto Nacional de Pesquisas Espaciais - INPE
Gabinete do Diretor (GB)
Serviço de Informação e Documentação (SID)
Caixa Postal 515 - CEP 12.245-970
São José dos Campos - SP - Brasil
Tel.:(012) 3945-6911/6923
Fax: (012) 3945-6919
E-mail: pubtc@sid.inpe.br

Research and development in a small Spherical Tokamak

G.O. Ludwig*, E. Del Bosco, J.J. Barroso, L.A. Berni, M.C.R. Andrade, J.G. Ferreira, R.M. Oliveira, P.J. Castro, J.O. Rossi, C.S. Shibata, R. Nayaranan, R.M. Castro

Laboratório Associado de Plasma, Instituto Nacional de Pesquisas Espaciais
12227-010 São José dos Campos, SP, Brazil

*E-mail: ludwig@plasma.inpe.br

Abstract This report presents a summary of activities carried out in the ETE spherical tokamak experiment and results obtained during the period 2005-2009. The main effort, besides theoretical and numerical modeling, has been in developing and installing diagnostic tools in the ETE tokamak, towards both a comprehensive study of plasma properties in the spherical configuration and examining the interplay between core and edge plasma properties. Also, some effort has been put into the technological development of high-power microwave sources for plasma preionization, and of diamond coatings for plasma-facing components. Pending upgrade of the power and control systems, the ETE experiment is presently equipped to carry on a modest, but hopefully fruitful, research program in the physics of spherical tokamaks.

Key words Spherical Tokamak, tokamak theory and modeling, plasma diagnostics, high power microwave sources, plasma facing components

Introduction

ETE (Experimento Tokamak Esférico) is a small spherical tokamak operational since the end of 2000 [20, 28]. The main parameters are: major radius R_0=30 cm; minor radius a=20 cm; aspect ratio A≈1.5; plasma current I_p=50~200 kA; pulse duration t_p=10~50 ms; magnetic field B_0=0.2~0.5 T; electron temperature T_e≈160 eV (without auxiliary heating); and plasma density $n_e \leq 3\times10^{19}$ m^{-3}. Figure 1 shows a general view of the ETE spherical tokamak. At present, the device performance is undergoing optimization and improved diagnostics are being installed. The ohmic system is temporarily operated in a low-energy single-polarity mode (plasma current ≤60 kA, duration ≤1 2 ms) while the capacitor banks' energy is gradually increased. The main research activities are: physics and technology of low aspect ratio tokamaks; plasma edge and plasma surface interaction studies; development of plasma diagnostics; and development of high-power microwave sources for plasma heating. The first part of this report describes the principal results obtained during the last few years in the areas of theoretical studies and modeling of plasma formation and sustainment, related to the present and future operation scenarios of ETE. The second part describes the development and improvement of diagnostic tools installed in ETE. Finally, the third part describes technological developments related to the ETE experiment, particularly in the area of high power microwave sources for preionization and plasma heating.

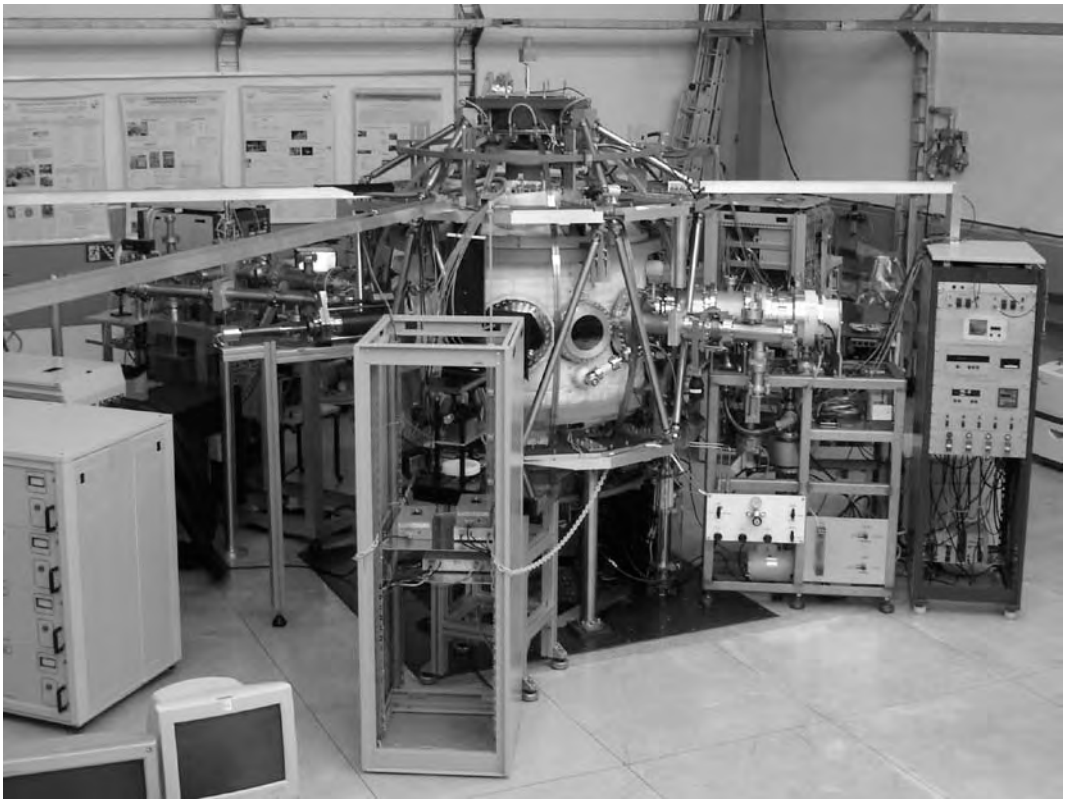

Fig. 1. General view of the ETE spherical tokamak experiment.

Studies related to plasma formation and sustainment

Startup

To simulate the plasma startup conditions, a model including all the external flux sources and eddy current effects in ETE has been developed, taking into account the eddy currents induced both in the central column and vacuum vessel wall, and the proximity effect of the ohmic solenoid. The ohmic solenoid impedance is calculated using eigenfunction expansions of the current distribution in the central column and in the solenoid [29] while the distribution of eddy currents in the vessel wall is calculated using a thin shell approximation [30]. Figure 2 shows diagrams of the penetration of the magnetization and equilibrium fields in the vessel wall at successive time instants. In the situation illustrated by Fig. 2 the ohmic and equilibrium circuits are switched on simultaneously, but without plasma formation. The left-hand side diagram in Fig. 2 corresponds to an instant τ_0 after switch-on and the right-hand side diagram to $5\times\tau_0$, where $\tau_0=\mu_0\sigma\delta a_V=1.23$ ms is the characteristic time defined by the product of the vacuum permeability μ_0, the conductivity of the Inconel walls $\sigma\approx7.8\times10^5$ $(\Omega m)^{-1}$, the effective wall thickness $\delta=4.85$ mm, and the minor radius of the vacuum vessel $a_V=25.9$ cm. The distribution of eddy currents induced in the vessel wall and the total electromotive force excited in loop voltage sensors placed along the poloidal perimeter of the vacuum vessel have been calculated, showing very good agreement with measurements performed in ETE [33]. Figure 3 shows a drawing of the ETE vacuum vessel and the distribution around the vacuum vessel wall of the loop voltage sensors used to test the eddy current model. A comparison is shown in Fig. 4 between the signals measured with the loop voltage sensors and the values calculated with the model, for a test shot of the magnetization field without plasma formation. Work will

continue in developing a full model to simulate the plasma startup conditions in ETE, including the eddy current model and testing different representations of the plasma. With this objective, a preliminary model was implemented using both an equivalent surface current description of the plasma current and a spectral representation of flux surfaces for simulating the equilibrium evolution of tokamak plasma coupled to various driving and eddy current external sources [37]. Figure 5 illustrates the preliminary results of this model. Tests of both filament and spectral descriptions of the plasma are being carried out in concomitance with the development of equilibrium reconstruction tools for ETE [3].

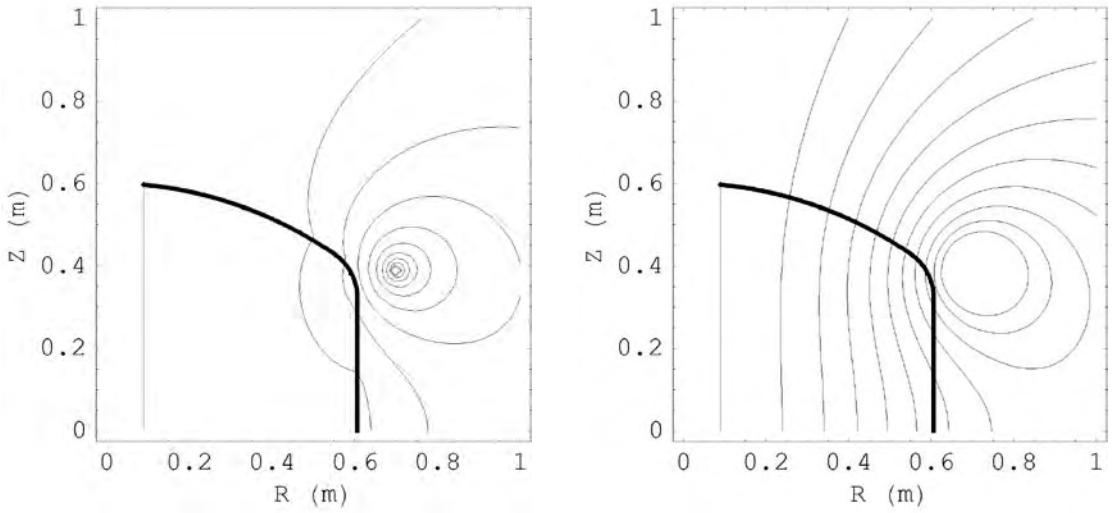

Fig. 2. Penetration of the magnetization and equilibrium fields in the vacuum vessel wall of ETE at two successive time instants.

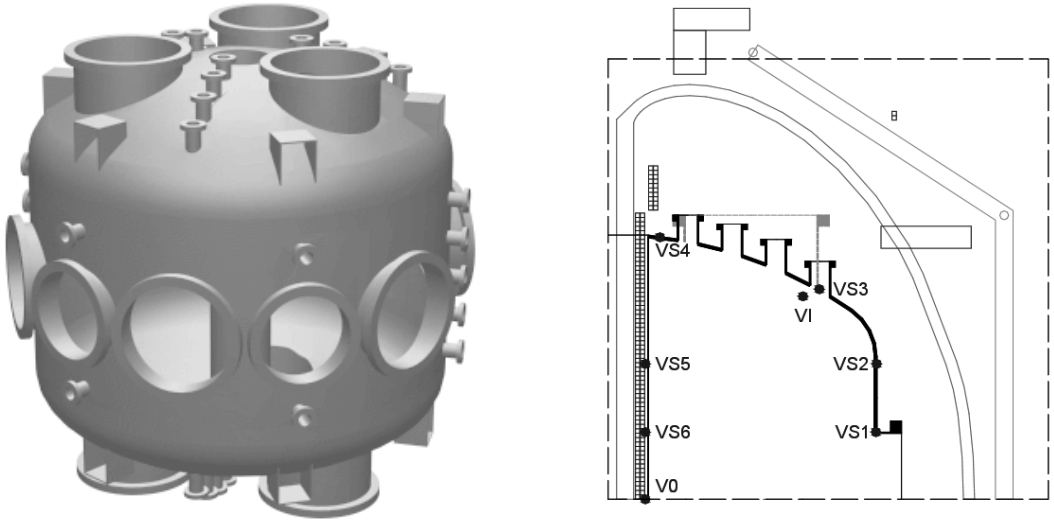

Fig. 3. Left: Drawing of the ETE vacuum vessel. **Right:** Location of the loop voltage sensors around the perimeter of the vacuum vessel wall.

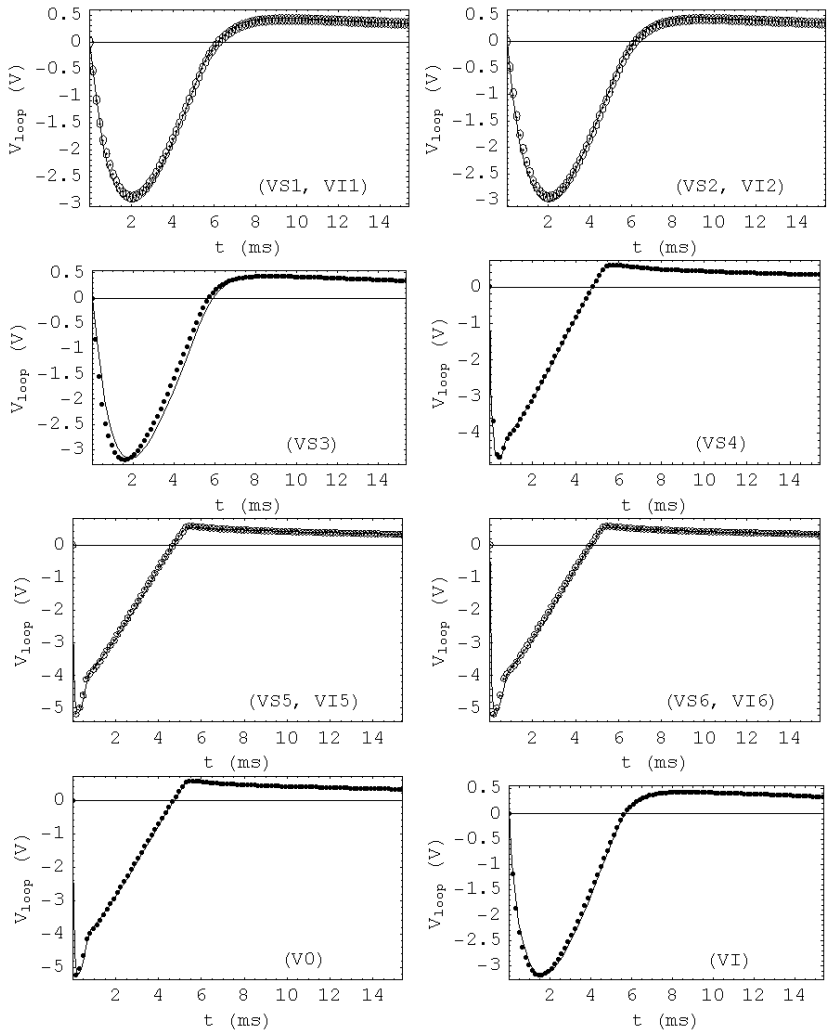

Fig. 4. Comparison between signals measured with loop voltage sensors (dots) and calculated with the eddy current model (lines). The only noticeable discrepancy corresponds to the loop voltage sensor VS3, which is not perfectly axisymmetric as assumed in the model. The loop voltage sensor VS3 was mounted flush to the large upper flanges tubes, as indicated schematically in the right-hand side panel of Fig. 3, bending around the small upper ports.

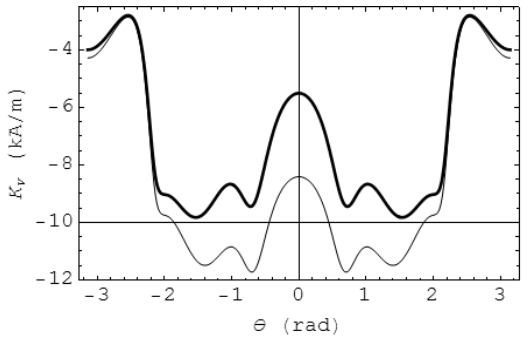

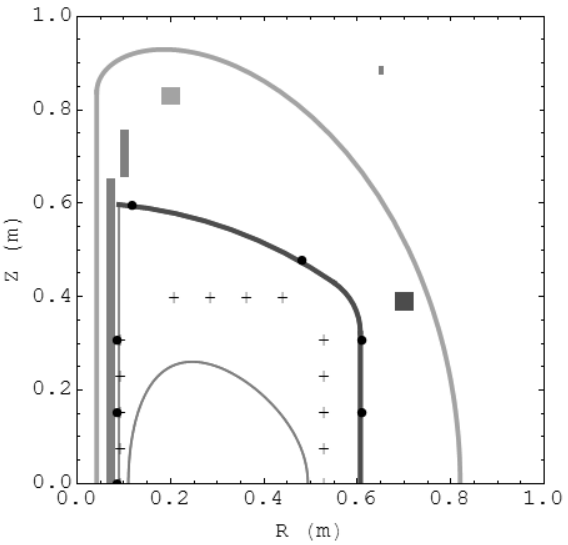

Fig. 5. Left: Surface current distribution in the vacuum vessel wall with plasma (thick line) and without plasma (thin line). **Right:** Theoretical reconstruction of the plasma shape at maximum plasma current. The figure also shows the centerlines both of the vacuum vessel wall and toroidal field coil, the profiles of the poloidal field coils, and the positions of the magnetic pickup coils (crosses) and flux loops (dots).

Steady-state operation

Simple dynamical models are needed to investigate the efficiency and time dependence of electron cyclotron current drive (ECCD) in different tokamak operating conditions. With this application in view, a fully relativistic fluid model for the energetic beam of current-carrying electrons has been developed [34]. Using a macroscopic approach, this model was applied to examine the efficiency of high-power current drive experiments, reproducing the main experimental features [35]. The calculated variation of the global figure of merit of ECCD versus the parallel refractive index showed good agreement with the DIII-D tokamak experimental results [42] as displayed in Fig. 6. Also, the model reproduced the variation of the perpendicular temperature of the high energy electrons with the parallel refractive index obtained in ECCD experiments performed in the TCV tokamak [19] as shown in Fig. 7. This model will be improved in several ways, mostly concerning trapped particle effects, and used to explore theoretically the interaction of the radiofrequency (RF) driven current with oscillating components of the inductive electric field.

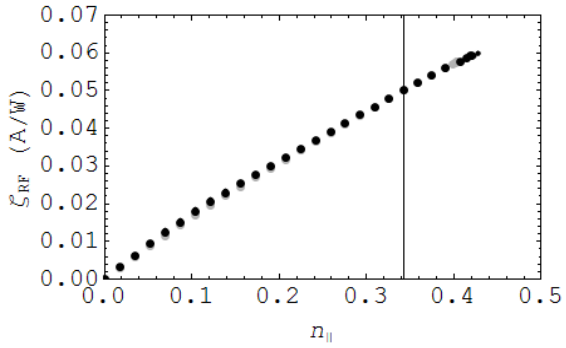

Fig. 6. Above left: Calculated global figure of merit versus the parallel refractive index for the DIII-D tokamak conditions. The vertical line corresponds to a toroidal injection angle φ_T=20° giving ζ_{RF}=0.05 A/W.

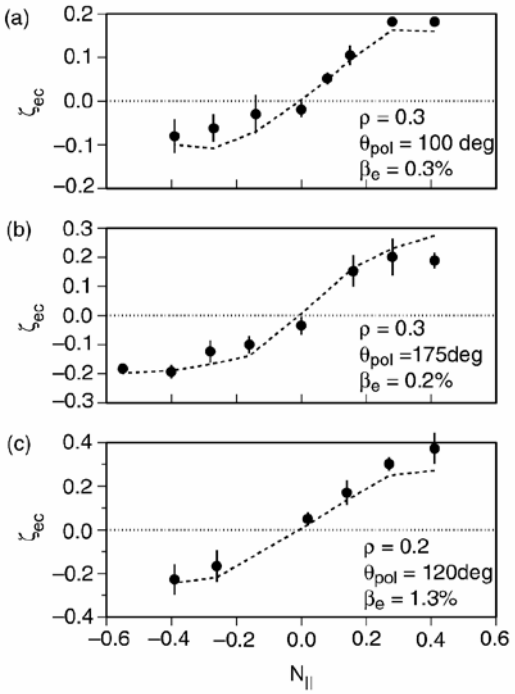

Right: Global figure of merit for the DIII-D tokamak ECCD experiment [42]. The model discussed in the present report does not take into account poloidal angle variations, but the calculated result ζ_{RF}=0.05 A/W for φ_T=20° corresponds to the experimentalist definition ζ_{ec} of the global figure of merit for θ_{pol}≈175° and φ_T=20°.

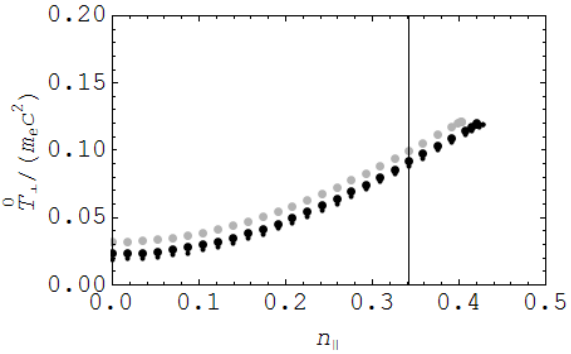

Fig. 7. Above left: Variation of the perpendicular temperature of the streaming electrons with the parallel refractive index in ECCD conditions similar to the toroidal injection angle sweeping experiment performed in the TCV tokamak. The calculated results indicate that for φ_T=0° and φ_T=20° the perpendicular temperature is $T_\perp \approx$12 keV and $T_\perp \approx$51 keV, respectively (note that $m_e c^2$=511 keV). The grey and black dots correspond to slight mismatches in the resonance condition with the wave angular frequency ω less than but approximately equal to the electron cyclotron frequency Ω_e.

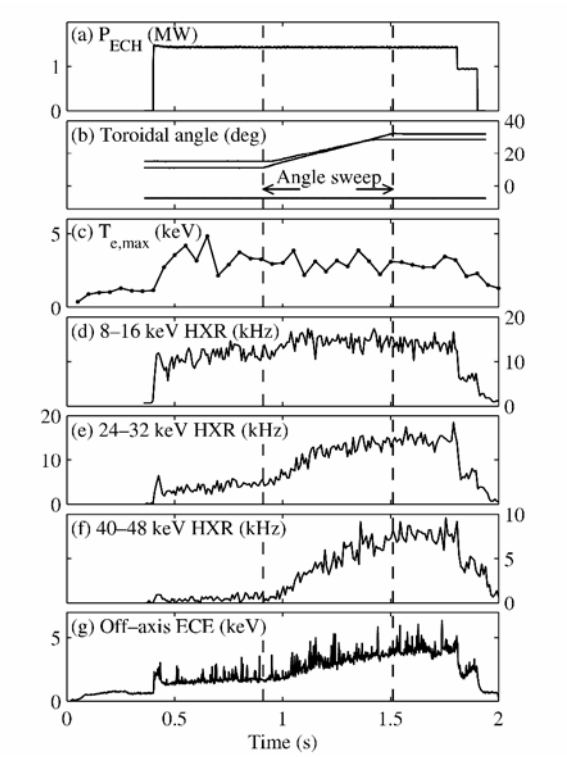

Right: Results of the ECCD experiment in TCV for a toroidal injection angle sweep in the range 12°<φ_T<30° [19]. The perpendicular temperature of the high energy electrons varies in the range 12 keV<$T_\perp$<50 keV (upper value limited by the detectors range), as shown by the energy resolved hard X-ray measurements.

Bootstrap current and neoclassical effects

Two equivalent scalings for the bootstrap current, based in theoretical considerations and on the analyses of this current response to variations of tokamak plasma profile parameters, effective charge, plasma geometry, magnetic field and plasma current, were obtained [1, 2]. These scalings are given for non-hollow profiles respectively in terms of beta normalized, cylindrical safety factor, internal inductance parameter and peakedness of the pressure profile, and as a combination of these parameters described in terms of both beta poloidal and pressure peakedness. This latter scaling for the ratio between the bootstrap current I_{bs} and the plasma current I_p is

$$I_{bs} / I_p = 0.234\, \varepsilon^{1/2}\, \beta_P\, c_p^{\,0.80},$$

where ε is the inverse aspect ratio, β_P is the poloidal beta, and $c_p = p(0)V(a)/\int p\, dV$ measures the peakedness of the pressure profile. Both formulations were obtained from a least-square fitting upon about 350 ETE calculated equilibria, in which some stability criteria were taken into account. Errors are mostly distributed up to the order of 10% when both expressions are compared with the equilibrium estimates for the bootstrap current in ETE. Figure 8 shows a comparison of scaling laws with equilibrium calculations. While the above scaling provides errors up to 10%, Hoang's scaling [25] provides errors up to 30% in relation to the equilibrium calculations performed for ETE.

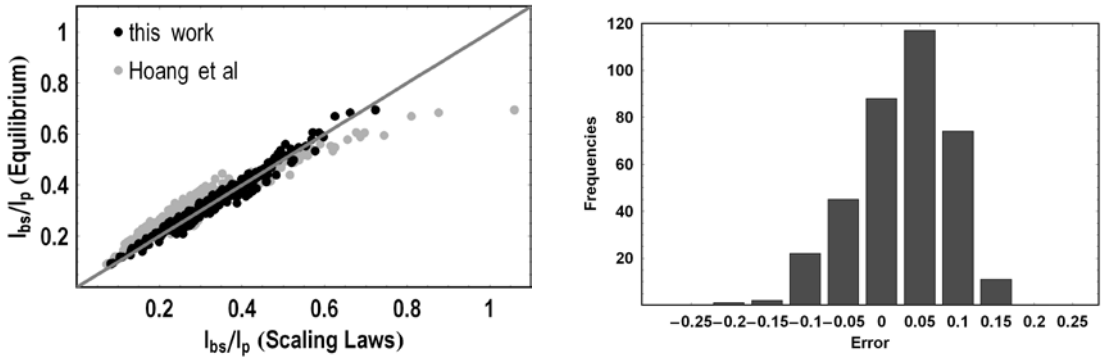

Fig. 8. Left: Comparison of scaling laws for the bootstrap current fraction with equilibrium calculations. **Right:** Histogram of errors for the ETE theoretical data set.

In parallel to the bootstrap current studies, an estimate of the plasma resistance in ETE was performed within the same equilibrium calculations. The neoclassical and Spitzer resistances have been estimated, being significantly different from the usual experimental value obtained from the measured loop voltage and total toroidal plasma current that includes effects not always associated with dissipative terms. The neoclassical resistance takes into account the presence of the bootstrap current and of the trapped particles, which modify the classical Spitzer value while in the Spitzer case these effects are not taken into account. A preliminary method has been proposed to relate the neoclassical and Spitzer values to the experimental value without having to solve the plasma equilibrium. It is interesting to remember that from the knowledge of the Spitzer resistance it is also possible to obtain a fast estimate of the plasma temperature. Indeed, in a preliminary application to ETE, the loop voltage measured with a flux loop around the solenoid in the central column is corrected to take into account plasma flux which is missed between the loop, at radius 4.35 cm, and the plasma inner border, at radius 5.0 cm. The inductive contribution is then subtracted from this corrected signal to produce the resistive loop voltage V_R, which finally gives the experimental (apparent) plasma resistance $R_{exp}=V_R/I_p$. Taking the average value $R_{exp}\approx 0.1$ mΩ during the shot and applying average neoclassical correction factors obtained from the equilibrium calculations the Spitzer resistance gives T_e=53 eV, close enough to the 60 eV value given by Thomson scattering measurements for the same shot. Neglecting neoclassical effects, i.e., taking $R_{Spitzer}=R_{exp}$, would produce T_e=46 eV. The main source of error in obtaining T_e by this method is believed to come from the separation of the resistive and inductive components of the loop voltage, which require good magnetic reconstruction of the plasma flux surfaces along the whole shot.

Plasma instabilities

Theoretical work has been carried out showing the influence of anomalous edge viscosity in the behavior of natural as well as laboratory plasmas [32]. In the case of natural plasmas the turbulence associated with the Rayleigh-Taylor instability, which is driven during the contracting stage of the decaying return stroke of a lightning discharge, creates anomalous viscosity that defines the spatial structure of bead lightning [31]. In the case of laboratory plasmas preliminary studies considered the kink mode instabilities in circular cylindrical plasmas taking into account the effect of viscosity in the boundary. It was shown that the m=1 kink mode is barely changed, but the higher order $m\geq 2$ modes are significantly damped if the collisionality is high. This has interesting implications for magnetic fusion, since the ballooning modes, which set a limit to the maximum pressure that can be confined in a tokamak, should be strongly

affected by viscosity. Furthermore, in the presence of flow at the edge viscous stresses are expected to modify the stability conditions, acting as a surface tension. The present macroscopic formulation could provide a simple description of this phenomenon, in a line of research that will be pursued in the future. Finally, in a recent investigation the ECCD fluid model described previously (in the subsection about steady state operation) was used to study the possible occurrence of the Weibel instability in the anisotropic electron stream driven in high-power current drive experiments. Figure 9 corresponds to preliminary calculations of the weak growth rate of the instability for the conditions of ECCD in the TCV tokamak, showing that the growth rate can have a maximum for a toroidal angle of injection $\varphi_T \approx 25°$.

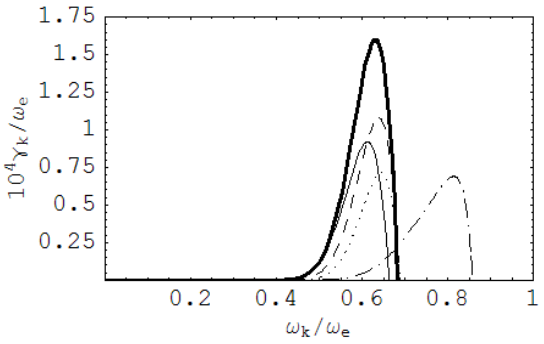

Fig. 9. Growth rate versus angular frequency of the Weibel instability normalized to the plasma frequency for an anisotropic suprathermal electron stream in the conditions of the ECCD experiment in the TCV tokamak. The curves give the growth rate for a toroidal angle of injection $\varphi_T=20°$ (dash dotted line), 22.5° (thin continuous), 25° (heavy continuous), 30° (dashed) and 35° (dotted). These results indicate that the Weibel instability has a maximum growth rate for a toroidal angle of injection $\varphi_T \approx 25°$.

Low-power reactors (Q≈1)

Simple global models are useful in performing a comprehensive analysis of fusion reactors. By means of a convenient normalization of the global power balance equation, it is possible to define a general figure of merit X, which depends on the energy confinement scaling law and encompasses all the relevant tokamak parameters [36]. In particular, the value of the figure of merit for ignition, $X_i \approx 1$, plays the role of an extended Lawson criterion. The figure-of-merit value was used to classify different hypothetical tokamak reactors and to analyze the performance of a class of newly proposed low-power reactors [23, 38]. These compact low-power devices represent an alternative route for the commercial viability of nuclear fusion, mainly if their use is dedicated to multi-functional ends as a hybrid fusion-fission machine, for instance. The performance of such machines was also analyzed using the ASTRA code, which is a very important tool on transport analysis in tokamaks. Collaboration for the use of the ASTRA code has been initiated with the Culham Science Center, situated in Abingdon, UK, with the inclusion in the code of the previously cited bootstrap current scalings (described in the subsection about bootstrap current and neoclassical effects). These scalings were also coupled with the simple global models to study the performance of fusion reactors. Preliminary calculations indicate the feasibility of low-power reactors with aspect ratio $1.6<A<2$, minor radius $a \leq 1$ m, magnetic fields $B \geq 2$ T and fusion gain $Q>1$, producing ~20 MW of fusion power with less than 500 kW/m^2 of wall loading on a close wall.

.

Diagnostics development and improvement

Core diagnostics

Thomson scattering (TS) is a well-established diagnostic for measuring electron temperature and density in fusion plasma experiments, with high spatial and temporal

resolutions. The initial one-channel TS system of the ETE spherical tokamak was successfully upgraded to a multipoint system based on the time delay technique of the collected scattered light from the plasma. This technique allows the utilization of one polychromator to collect the light of several points in the plasma core in one single shot, reducing the cost of the conventional multipoint TS system. Firstly the technique was successfully tested in ETE for four channels [14, 15], and then upgraded to ten channels. Because the effective area of the detection system is limited to 7 mm^2 it was not possible to introduce more than ten fibers inside the present polychromator. The scattered light is imaged by a collection lens set (numerical aperture NA=0.07) on ten large core monofibers (diameter=0.8 mm, NA=0.39, attenuation=7 dB/km) of different lengths (fiber number 1 with a length of 8 m and fiber number 10 with a length of 134 m) to relay the light signals to the same polychromator. Between the collection lens and each monofiber a microlens (focal length=15 mm) was placed to match the numerical aperture of the optical system and to enlarge the observation length inside the plasma to 4 mm. Figure 10 shows images of the light collection optics and of the stack of fiber optics reels forming the delay line of the 10-channel TS diagnostic. Figure 11 shows the delay time and transmission for each channel of the 10-channel TS diagnostic. Illustrating the use of the multipoint TS system, Fig. 12 shows radial profiles of the temperature and density obtained at a given instant for a shot in the ETE tokamak. Recently, improvements concerning the signal to noise (S/N) ratio have been attained by ray-tracing simulations comprising all parts of the Thomson scattering optical system as illustrated by Fig. 13. The scattering profiles used for the rough surfaces involved (steel, inconel, aluminum and graphite) were measured in laboratory in order to have near realistic results. The simulations showed that for an output laser energy of 10 J the dump reflects back 0.96 J. The stray light at the collection window amounts to 4 mJ, with contributions from the chamber, central column and dump equal to 3.7 mJ, 0.2 mJ and 0.1 mJ, respectively. Practically, the stray light contribution from the flight tube is null. These results indicated that the amount of energy reflected back from the dump should be reduced to diminish the effect of stray light at the collection lens. This was accomplished through a redesign of the internal components of the dump as shown by Fig. 14. The energy reflected back from the dump was reduced from 0.96 J to 3.7 mJ resulting in a significant decrease of the stray light at the collection window from 4 mJ to 10 μJ. The stray light reduction was confirmed by measurements at several internal points on the poloidal cross-section of the vacuum chamber [16].

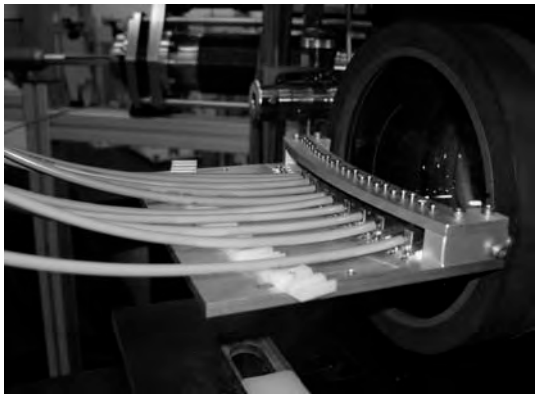

Fig. 10. Above: Light collection optics of the 10-channel Thomson scattering (TS) diagnostic. **Right:** Stack of fiber optics reels forming the delay line of the 10-channel TS diagnostic.

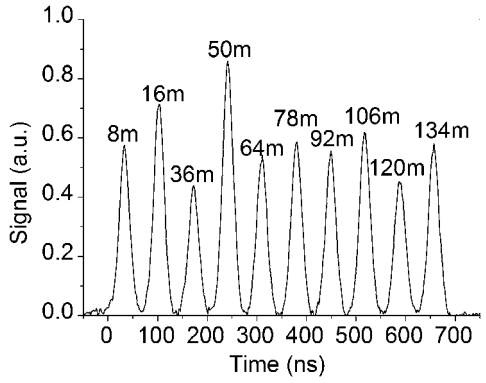

Fig. 11. Delay time and transmission for each channel of the 10-channel TS diagnostic. The length of each optics fiber is indicated.

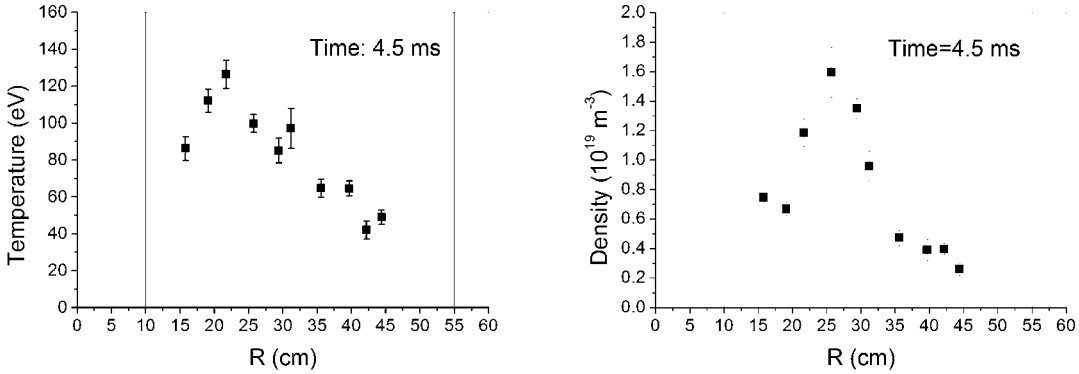

Fig. 12. Left: Radial temperature distribution obtained for an ETE shot using the multipoint TS system. **Right:** Radial density distribution obtained for the same ETE shot. The vertical lines correspond to the positions of the graphite limiters.

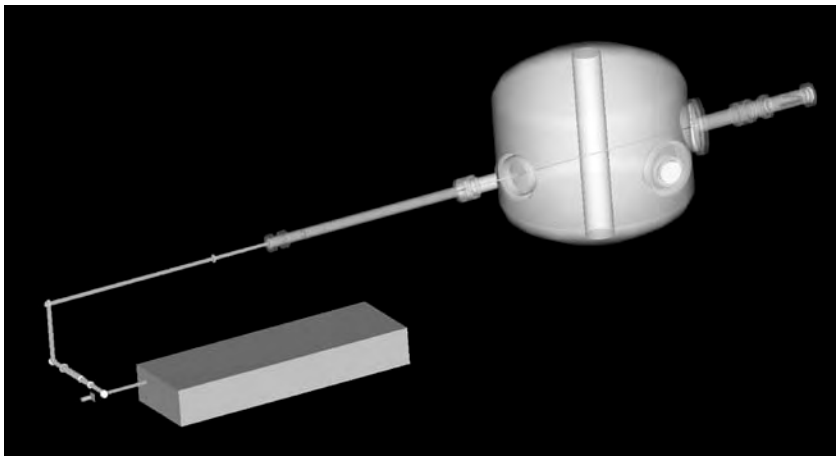

Fig. 13. Layout of the Thomson scattering high-intensity laser and vacuum chamber system in the ETE spherical tokamak. The laser energy dump is depicted on the far right-hand side of the figure.

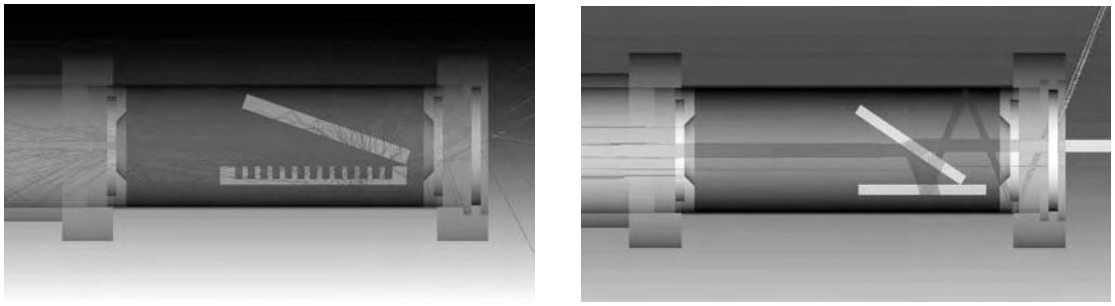

Fig. 14. Left: Schematic of the initial laser energy dump. **Right:** Improved laser energy dump.

A one-chord interferometer using Mach-Zehnder geometry and a heterodyne detection setup was installed in the ETE spherical tokamak. The interferometer operates at a fixed frequency of 170 GHz (λ~1.8 mm) and the microwave beam probes the ETE plasma at a vertical chord. For this initial setup it is possible to choose two chords (R=30 cm or R=39 cm) that can be changed between shots. The microwave beam is guided by a WR-06 line and connected to the ETE vessel by a WR-28 horn through fused-quartz windows. Special shutters prevent the damage of the quartz windows both from the glow discharge cleaning procedure and from the plasma when the diagnostic is not operating. Figure 15 shows a picture of the microwave interferometer and the density profile in ETE for a short test shot of the interferometer.

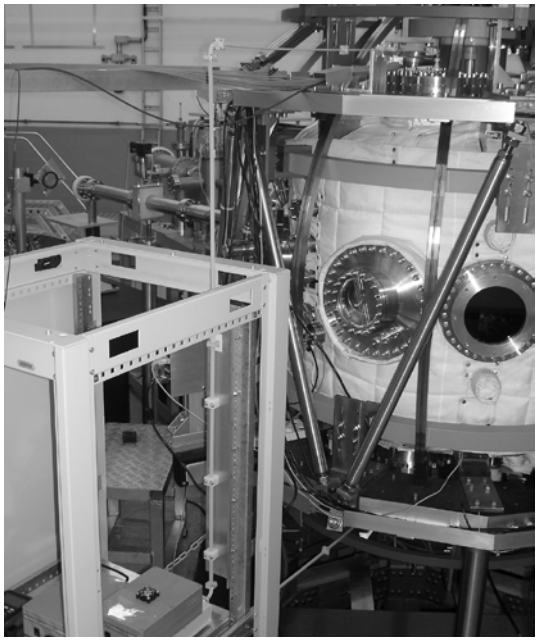

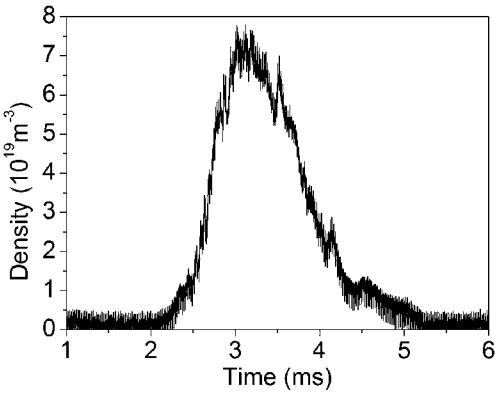

Fig. 15. Left: Picture of the 1.8 mm microwave interferometer. **Right:** Trace of the plasma density in ETE at R=30 cm obtained for a short test shot with the interferometer.

In ETE discharges the presence of runaway electrons, which is a common phenomenon in tokamaks, is usually monitored using a *NaI(Tl)* scintillator detector. This measurement technique gives information about the losses of highly energetic particles to the limiter target or chamber wall (target bremsstrahlung). Now, the runaway production rate coefficient λ_r [21, 22], which is a function of the ratio of accelerating electric field to the critical electric field necessary for generating runaway discharges E/E_c, is estimated using the Thomson scattering data of Fig. 12 at several radial positions as shown in Fig. 16. These plots indicate that the favorable conditions for runaway electrons generation are in regions away from the centre of the plasma and towards the edges. Nevertheless, the actual production will also depend on the electron temperature and density profiles, generally concentrating the runaway production in the center of the discharge. Since most of the present ETE discharges show runaway electrons in different conditions, it is necessary to understand the core-to-edge runaway formation and dynamics in a better manner. Furthermore, the dynamics of runaway electrons, which are essentially collisionless, provides useful information about the mechanisms involved in anomalous particle transport in tokamak plasmas. In order to get a better understanding of the evolution of these highly energetic electrons inside the plasma cross-section, before they are lost to the limiter, it is planned to install a set of *CdTe* detectors (EURORAD 2mm×2mm×2mm) inside the vacuum vessel of ETE. The advantage of using these semiconductor detectors is that they are not only compatible to

vacuum and insensitive to large magnetic fields but also have a relatively low pulse rise time and high stopping efficiency [43]. These detectors have good detection efficiency from a few keV up to 120~170 keV. With this application in mind, a prototype *CdTe* detector system was recently tested outside the ETE vacuum vessel and the obtained signals were compared with hard X-ray emissions registered by two scintillator detectors [39]. Figure 17 shows some results of this comparison. Presently, the electronics circuitry is being improved in preparation for assembling the full set of *CdTe* detectors as soon as they are purchased. Taking into account the present ETE operating conditions and the sensitivity of the detectors being ~0.4 mV/keV (8 mV at 20 keV), the *CdTe* detector system will not be feasible for free-free bremsstrahlung measurements in the hard X-ray regime (> few tens of keV), because of the low photon counts available. Therefore, the system will be used initially for measurements in the soft X-ray regime, using cut-off filters at low energies (~1 keV), or in the hard X-ray range by introducing a set of targets at different radial locations inside the plasma. As the operating conditions in ETE improve, the detector system can be used for measurements in higher energy ranges, by simply changing the low energy cut-off filters.

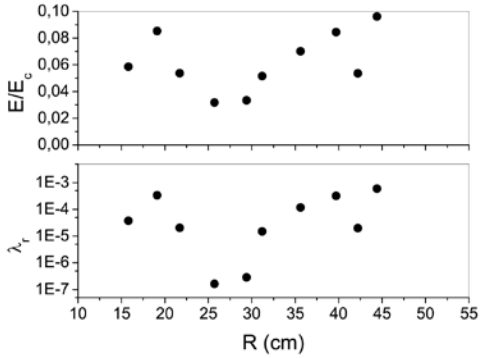

Fig. 16. Estimated parameters in regions of primary runaway generation using the Thomson scattering data of Fig. 15: (a) ratio between the accelerating electric field and the critical electric field required for runaway generation (E/E_c); (b) production rate coefficient of primary runaway electrons.

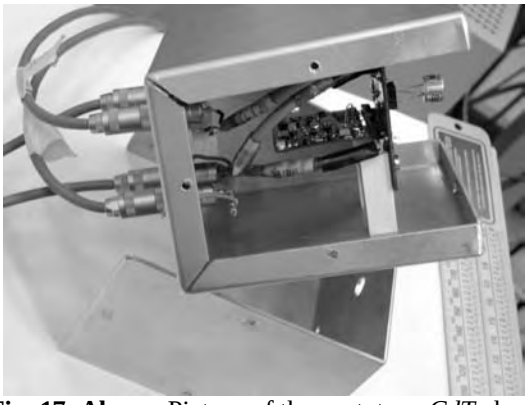

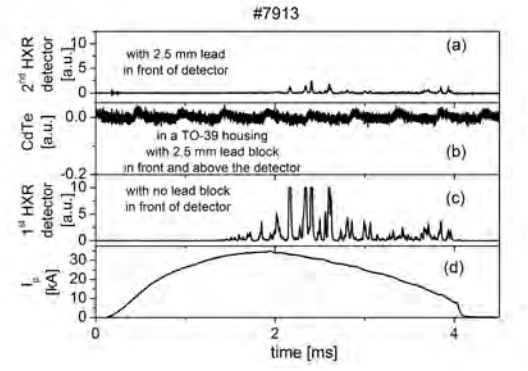

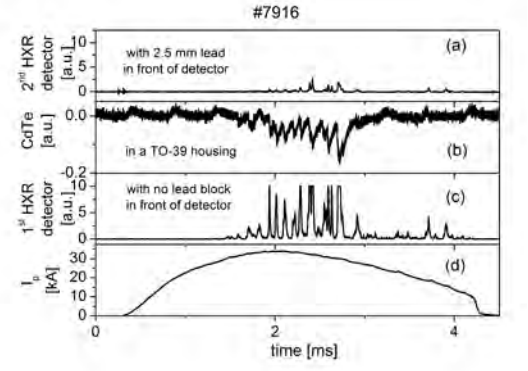

Fig. 17. Above: Picture of the prototype *CdTe* hard X-ray (HXR) detector. **Top right:** Response of the *CdTe* (b), and 1st (c) and 2nd (a) scintillator detectors to limiter bremsstrahlung radiation in short plasma discharges (d). The 2nd scintillator (a) and the *CdTe* (b) detectors had a 2.5 mm lead block in front of them, whereas the 1st scintillator (c) detector was kept without any additional shielding. **Bottom right:** Same as in the top figure, but with the lead block removed from the front of the *CdTe* detector. There is a good correspondence between the *CdTe* and 1st scintillator detectors responses. The minimal variation of the 1st and 2nd detectors between shots was independently tested.

As part of the effort in developing tools for plasma core diagnostics, a set of five silicon photodiode detectors (AXUV-100-IRD 10mm×10mm) was procured and tested in the ETE environment. These soft X-ray detectors will be used for the determination of the electron temperature with high time resolution, and as a test for a planned tomographic imager. A prototype soft X-ray camera using one silicon detector was assembled in a vacuum flange with a slit opening of 5 mm×2 mm and a 10 μm *Be* filter. Figure 18 shows the position of the prototype soft X-ray camera with respect to the ETE vacuum vessel. Figure 19 shows a picture of the prototype camera and a comparison of the radiation signals in the soft and hard X-ray ranges obtained with the soft X-ray camera and the hard X-ray scintillator, respectively [39]. The electron temperature values in the soft X-ray range will be validated by the Thomson scattering measurements. Recently, a set of two arrays with sixteen silicon sensors on each array (AXUV-16EL-IRD 2mm×5mm(×16)) was purchased to initiate the development of tomographic cameras in the soft X-ray range.

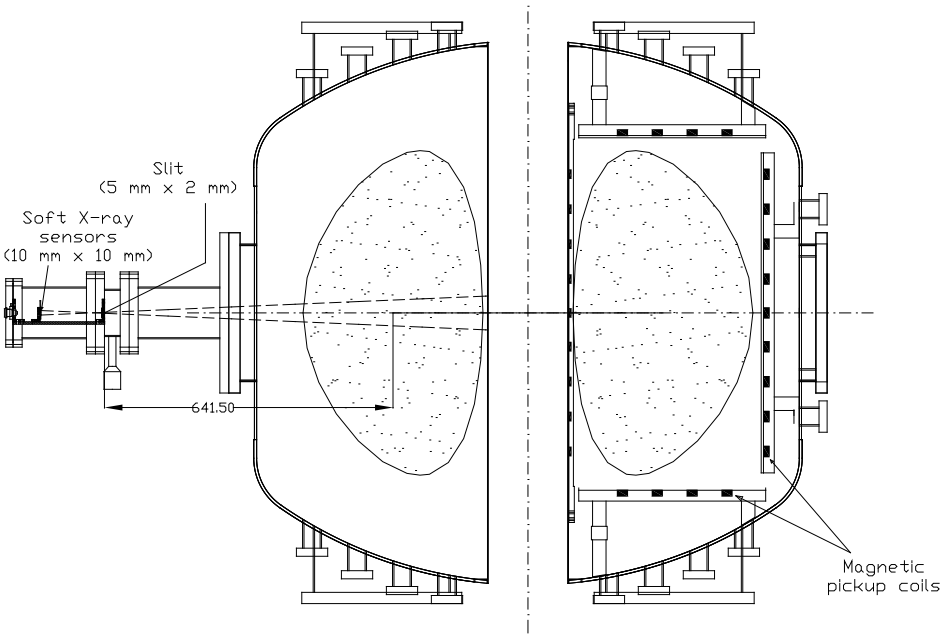

Fig. 18. Positions of the prototype soft X-ray camera (left) and magnetic pick-up coils (right) with respect to the ETE vacuum vessel.

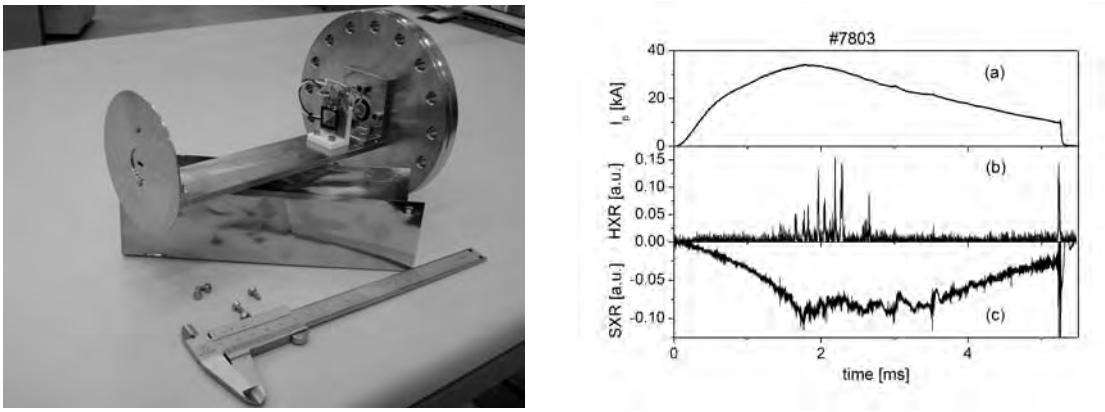

Fig. 19. Left: Picture of the prototype SXR camera. **Right:** Response of the hard X-rays scintillator (b) and soft X-rays silicon detector (c) to limiter and thermal bremsstrahlung radiation, respectively, emitted by a short plasma discharge (a).

Finally, on the subtopic of core diagnostics, a visible light spectrometer (12 A°/mm) for *CIII* impurity emission detection and a *Hα* detector with interference filter ($\Delta\lambda$ = 13.52 nm) have been routinely used. One fast CCD B&W camera with speeds up to 500 FPS has been used on loan during the first operation phase of ETE. Presently, two fast CMOS color cameras with speeds up to 8000 FPS are being purchased.

Edge diagnostics

An upgrade of the 10 keV fast neutral lithium beam (FNLB) probe was performed after successful measurements of the temporal evolution of plasma density in the ETE tokamak discharges [40, 41]. Figure 20 shows a picture of the neutral lithium beam line and a signal of the plasma density measured at the edge with the initial setup of the diagnostic. For upgrading, the main modification concerned the replacement of the initial one-channel optical detection system by an eight-channel system. The high spatial (1 cm) and temporal (tens of nanoseconds) resolutions previously achieved were retained. With the new system the density profile at the plasma edge can be obtained in a single shot, using an appropriate calibration method for plasma density determination. Figure 21 illustrates the calibration curves obtained in hydrogen for four channels of the detection system. The vacuum window used for observations of the light emitted from the plasma, as a result of interaction with the lithium beam, allows visualizing a 15 cm radial length of the plasma from the edge. A narrow 1 nm pass-band interference filter separates the measuring wavelength of interest (670.8 nm) from the background light. A set of nine optical fibers, each one with a 1.5 mm diameter single encapsulation, and 99.8% transmission rate per meter at 670.8 nm, guides the emitted light to the multi-channel photomultiplier, which composes a frame of 8×8 cells. Parallel connection of eight cells allows gain amplification by a factor of eight, in comparison with the case of using just one cell for each observed radial position. Preliminary measurements of the fast varying pressure inside the vacuum chamber due to gas injection by puff valves were performed, as also shown in Fig. 21. Pending additional calibration and optimization, the overall system is ready to initiate measurements of the plasma density and its fluctuations during discharges in ETE, bringing relevant edge plasma information to present research performed in spherical tokamaks.

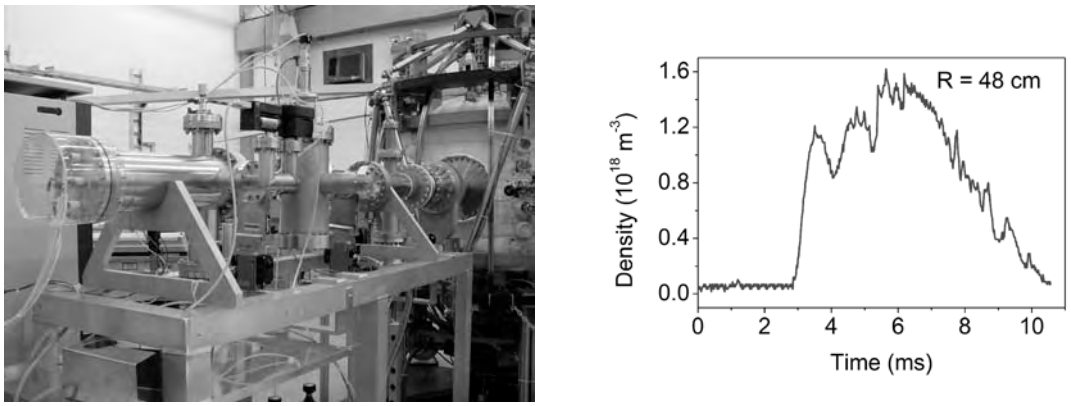

Fig. 20. Left: 10 keV fast neutral lithium beam line (FNLB). **Right:** Plasma density measured with the FNLB probe in the edge of ETE at 7 cm from the outboard limiter.

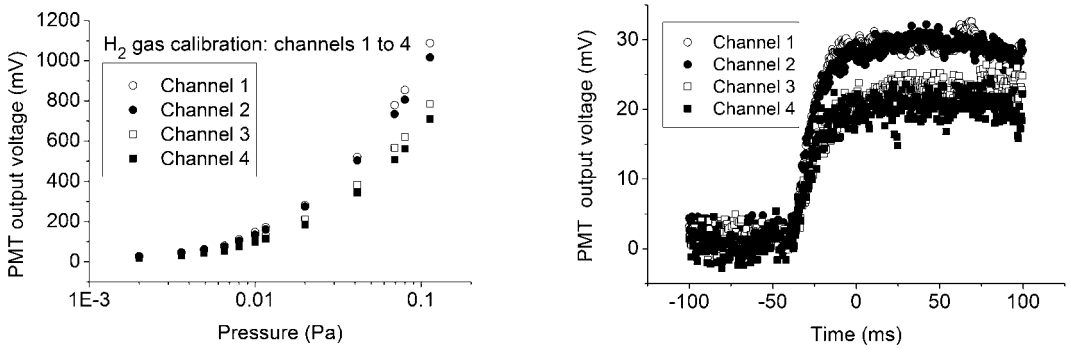

Fig. 21. Left: Hydrogen calibration curves for channels 1 to 4 of the FNLB probe detection system. **Right:** Raw signals corresponding to a gas puffing test. Channel 1 corresponds to the outer edge of the plasma and channel 4 to a position 15 cm inward. Channels 2 and 3 are at equally spaced intermediate positions. Although cluttered by the symbols in highly fluctuating signals, this figure shows that the average values should coincide after calibration according to the left-hand side plot.

A set of magnetic sensors (pickup coils, Rogowski coils, total flux coils) for magnetic measurements and equilibrium reconstruction studies was fabricated and installed inside the ETE vacuum vessel. The first set of magnetic sensors already assembled consists of: twenty six two-component fixed probes; one two-component movable probe at Z=0; two total Rogowski coils (one inside and the other outside the vacuum vessel); four partial Rogowski coils; and eleven total flux loops outside, plus one inside the vessel. These sensors are mostly assembled in one sector of the limiter from a total of eight sectors. Additional sensors will be installed with the complete eight sectors limiter comprising six partial flux loops (saddle coils), six total flux loops inside the vessel, and four two-component probes at Z=0 but different toroidal angles. Figure 22 shows a picture of the total and partial Rogowski coils and the two-component pick-up coils mounted inside one sector of the inner wall limiter, a picture of a set of the two-component pick-up coils assembled in the upper arm of the graphite limiter showing part of the shielding, and a picture of the output connections of the first set of magnetic sensors. These magnetic diagnostics make extensive use of a 64-channels data acquisition system based on the PCI standard that was integrated by the Centro de Fusão Nuclear (CFN), Instituto Superior Técnico (IST) in Lisbon, Portugal. This data acquisition system was recently upgraded to 256-channels, to accommodate all the magnetic coils signals plus new diagnostics that are ready to be installed in ETE.

In the present setup, the pickup coils outputs are connected directly to the data acquisition system. The pickup coils signals, obtained in such a manner, are observed to have a maximum output voltage of 1 V. With the maximum range of the data acquisition system input being 10 V, there is a plan for installing a buffer electronic amplifier circuit at the output of the coils in the future. The data acquisition is triggered 1 ms prior to the initiation of the toroidal field coil capacitor bank. This is done to keep a record of the toroidal field coil current evolution during a discharge as well as to get an estimate of the initial signal levels in the pickups coils, both from the externally discharged coils and the resulting eddy current effects induced in the vacuum vessel. The signals from these external sources must be subtracted from the actual plasma discharge effects. This is done by measuring the pickup coil signals with similar initial capacitor bank voltages and trigger timings as that of the plasma discharge in question but without any gas puff introduced into the chamber. However, it is to be noted that this method of subtraction has its own pitfalls. It does not take into consideration the feedback effects on the external coils and eddy currents due to the presence of the

plasma component, as well as the resultant change in evolution of the external sources after the termination of the plasma discharge. Another source of error is the shot to shot variation in the applied fields, including the toroidal field coil current. However, keeping these errors in mind, the subtraction method still gives a good estimate of the plasma evolution related magnetic field pickup signals along the rectangular cross-section of the coil. A full model of the eddy current effects, taking into account the coupling between the plasma and the external sources is being presently developed [3, 37], as already mentioned in the subtopic about startup studies in ETE.

Fig. 22. Top left: Total and partial Rogowski coils, and two-component pick-up coils mounted inside one sector of the inner wall graphite limiter. **Bottom left:** Set of pick-up coils assembled on the upper arm of the limiter showing part of the shielding. **Right:** Output connections of the magnetic sensors.

In an initial step of magnetic reconstruction using experimental data, the plasma position has been estimated using the multipole moment expansion technique [18, 27, 46]

$$Y_m = I_p^{-1} \int j_\phi f_m \, dS_\phi = (\mu_0 I_p)^{-1} \int [f_m B_t + (R_0+\zeta) g_m B_n] d\ell,$$

where, Y_m is the m^{th} multipole moment; I_p is the plasma current and j_ϕ is the toroidal current density; f_m and g_m are two given functions of the radius R and coordinates (x, z); B_t and B_n are respectively the tangential and normal components of the magnetic field outside the plasma on the contour ℓ surrounding S_ϕ. The plasma coordinates are denoted by (x, z) whereas the contour coordinates are denoted by (ξ, η). The moments Y_0 and Y_1 give the plasma current and position, respectively. The experimental data obtained from the set of the two-component magnetic pickup coils have been employed to determine the evolution of the plasma position (Fig. 23), using the rectangular contour calculations of Shkarofsky's paper [46]. Figure 23(a) shows three discharges, namely shots nos. 7219, 7230 and 7255 with B_0=0.196 T for all three discharges. Shots 7219 and 7230 were obtained on the same day with the former being a discharge before a ten minute glow was carried out in the ETE vacuum chamber and the shot 7230 being a discharge obtained after the glow discharge. Shot 7255 was a discharge obtained on a subsequent day after a 30 minute glow discharge. The extension of the discharge duration from 3 ms to 5 ms, gives an indication of the importance of glow discharge for cleaner and better plasma. The plots of the horizontal, Δ_h, and vertical, Δ_v, displacement of the

plasma column during the temporal evolution of the three plasma discharges are plotted in Figs. 23(b) and (c), respectively. The convention followed for the displacement is that for a positive value of Δ_h and Δ_v the plasma position is located outwards and upwards with respect to the geometrical major radius (R_0, *0*). The plasma discharges used for estimating the density and temperature profiles in Fig. 12 are similar to that of shots 7230 and 7255. As has been observed from the Thomson scattering diagnostic results (Fig. 12), the ETE discharges tend to be shifted slightly towards the inner side of the vessel (40~50 mm). This is corroborated by the estimates of the horizontal plasma position from the magnetic pickup coil signals, as shown in Fig. 23(b). The ETE plasma also tends to be slightly shifted upwards (10~15 mm).

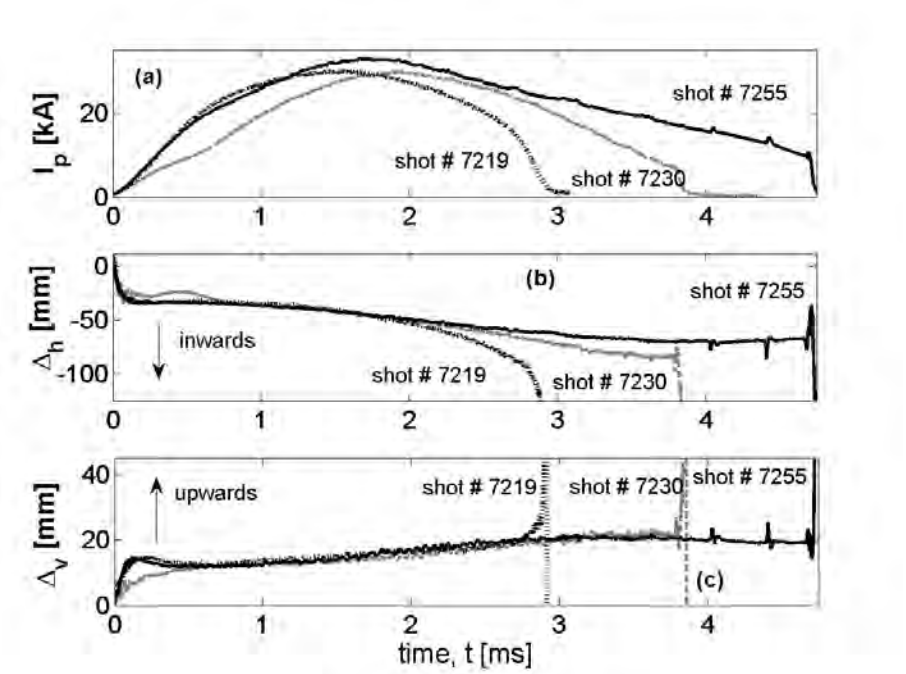

Fig 23. Plot of three ETE plasma discharges under same initial capacitor bank voltages (toroidal field B_0=0.196 T): (a) Plasma current I_p; (b) Horizontal plasma displacement Δ_h; (c) Vertical plasma displacement Δ_v.

Edge plasma cross-field transport properties are dominated by edge turbulence. These studies require the knowledge of parameters such as the plasma density, electron and ion temperatures, plasma potential, magnetic fields and flows as well as their fluctuation levels. A set of electrostatic probes has been installed in ETE to characterize the edge plasma behavior in conjunction with the magnetic sensors and the deep edge density fluctuations that can be detected with the FNLB probe. The set of electrostatic probes consists of one bellows vacuum sealed double probe, one single probe, and one cluster of nine Langmuir probes. All probes are movable. Figure 24 shows a picture of the bellows vacuum sealed movable double probe and a schematic of the cluster of nine probes. Preliminary measurements of the plasma edge parameters such as temperature and density were obtained from the characteristic curve $I=f(V)$ of the single Langmuir probe, where I is the measured current and V is the voltage applied to the probe. A high frequency sweeping-probe system is used to apply a fast triangular voltage waveform to the probe, and a dedicated computer program obtains the plasma temperature and density from the processed current signal. Figure 24 also shows both the time evolution of the plasma temperature and density and the radial profile of these plasma parameters obtained from the probe curves measured inside the plasma at a distance 10 mm beyond

the limiter. The cluster of nine Langmuir probes is presently being used to analyze plasma density fluctuations at the edge.

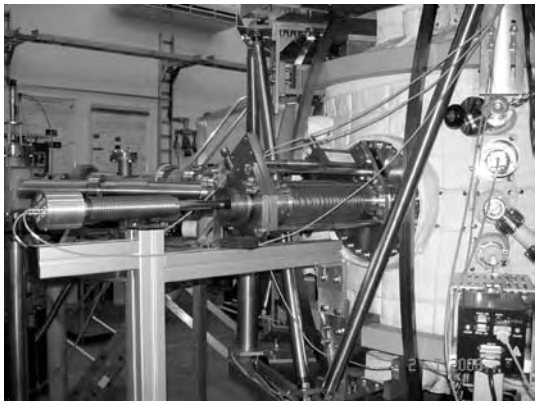

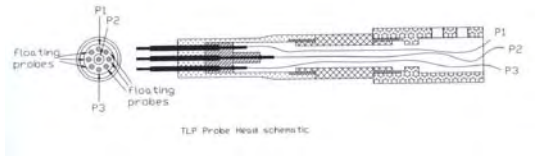

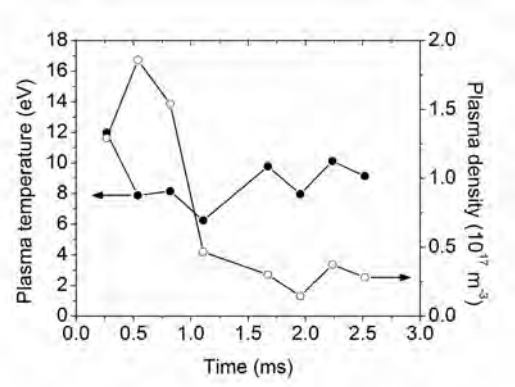

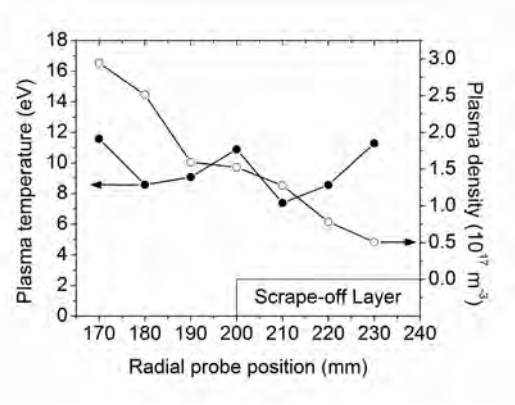

Fig. 24. Top left: Picture of the bellows vacuum sealed movable double Langmuir probe. **Bottom left:** Schematic of the cluster of nine movable Langmuir probes. **Top right:** Time evolution of the temperature and density inside the plasma at a distance 10 mm beyond the limiter. **Bottom right:** Radial profiles of the plasma temperature and density at the plasma edge.

Technology developments

High-power microwave sources

The simplest of the microwaves tubes, a monotron, has been designed and constructed to operate at 6.7 GHz, a frequency suitable for plasma heating, communications, medical and industrial applications. The device shown in Fig. 25 includes an electron gun that accelerates and injects a hollow electron beam into a cylindrical cavity [17, 5] leading to the expected generation of 10 kW output RF power at typical 20% conversion efficiency. With inner and outer diameters of 5.2 cm and 6.0 cm, respectively, the hollow beam is emitted from an annular nickel strip with surrounding electrodes tipped at the Pierce angle of 67.5° toward the anode. The circular nickel strip is coated with a *(Ba, Sr, Ca)O* film that at the operation temperature of 800°C can provide a pulsed emission current density of 3.0 A/cm^2 [11]. Typical 5.0 A beam currents with duration 45 μs at a repetition rate of 50 Hz have been measured in high-voltage emission tests as also shown in Fig. 25, preceded by exhaustive thermal tests from which the overall thermal performance of the electron gun had been improved.

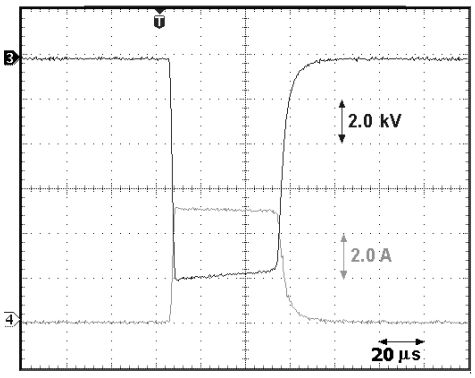

Fig. 25. Left: Full monotron mounted on a CF150 vacuum flange. The assembly includes the injection electron gun shown in the middle part of the picture, and the resonant cavity coupled through a circular hole to the TM-mode output waveguide shown in the top part of the picture. **Right:** Test of the high-voltage and high-current power supply with single tetrode.

Instead of dealing with a monoenergetic beam of electrons being injected at a prescribed energy into the cavity as in previous conceptual studies, more realistic particle-in cell (PIC) simulations of the monotron interaction have been performed by considering both of the processes of beam formation and acceleration by the electron gun as shown in the left panel of Fig. 26, which incorporates the complete layout of the 6.7 GHz monotron. The assembly includes an injection electron gun and a resonant cavity coupled to the TM-mode output waveguide through a circular hole. The cathode arrangement is devised to bend the equipotential surfaces so as to confine and focus the beam even in the presence of space-charge forces as the electrons move away from the emitting surface. Without divergence, the beam is injected into the cavity through an annular slot. In the bottom left panel of Fig. 26, it is shown the electron beam bunched in the steady–state regime, in which DC beam power is converted into electromagnetic power at a typical 20% conversion efficiency. The right panel of Fig. 26 shows the cold-test bench of the monotron [17]. The measurements indicated an overall power loss of 0.5 dB for the assembled test transmission line.

To meet high-power monotron operation, a high-voltage and high-current power supply (10 kV, 3×8A) has been designed on the basis of an innovative scheme illustrated by Fig. 27 in which three high-power tetrodes are connected in parallel [44, 45]. In this scheme, the high voltage switch and its grid power supplies are near the ground, which eases the maintenance and the pulser construction. In fact, the on-off switching uses a power MOSFET in series with the cathodes of three tetrodes of 8A maximum plate current each connected in parallel. This type of circuit configuration is very convenient because the tubes withstand the major fraction of the blocking voltage as IGBTs operate at maximum voltages up to 1.5 kV and they do not require high power gate drivers.

Tests of the monotron electron injector gun will continue with replacement of the nickel cathode by a new one made from tantalum. Also, the performance of the high-voltage and high-current power supply will be improved by incorporating two additional high-power tetrodes to meet the full specification. If successful, this development will lead to a microwave source for preionizing the plasma in ETE.

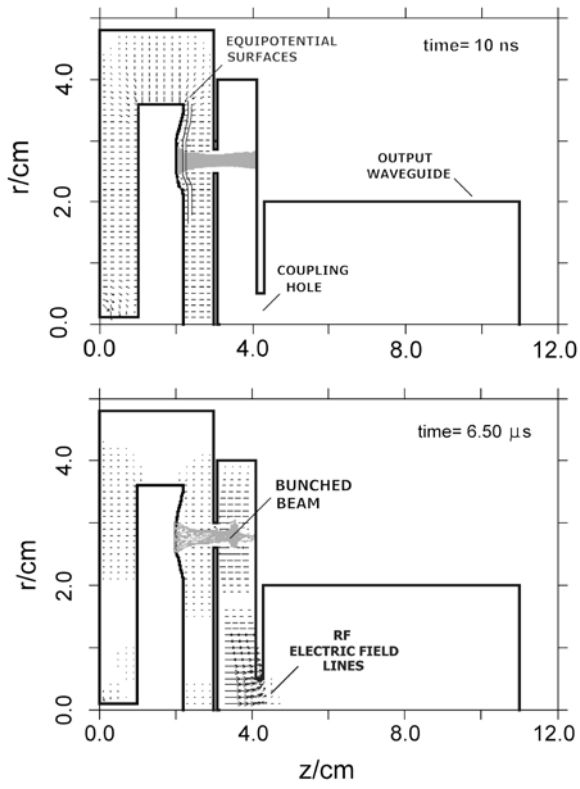

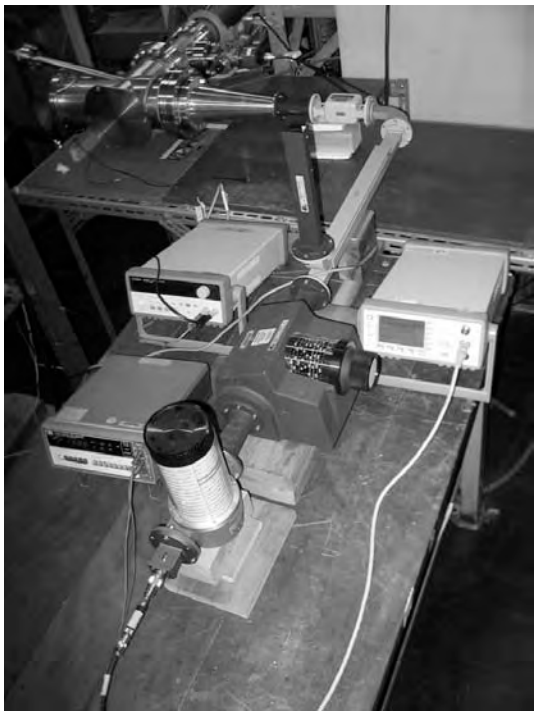

Fig 26. Left: Particle in cell simulation of the full monotron. **Right:** Cold test bench of the monotron.

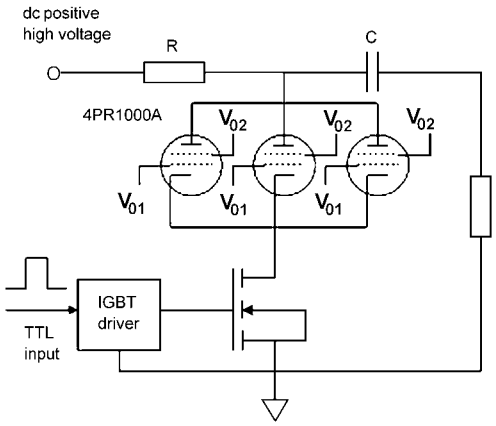

Fig. 27. Left: Schematic of the improved monotron power supply (10 kV, 3×8 A) using three tetrodes in parallel. **Right:** Picture of the monotron high-voltage and high-current power supply

On the theoretical side, conceptual studies have come to indicate that the monotron interaction can achieve conversion efficiency as high as 55% by considering a stepped axial electric-field profile along the electron stream [4]. The model uses two circular TM cavities coupled capacitively by an annular slit. Both cavities are carefully tailored so that the smaller cavity pre-modulates the beam while the second and larger resonant cavity provides the main interaction space. Moreover, an excitation model has been developed for TM-mode cylindrical cavities driven by a modulated hollow electron beam. The analysis begins with energy conservation considerations yielding an RC circuit-like equation that describes the evolution of the slowly time-varying

amplitude of the RF oscillations. It is shown that the slowly time varying amplitude of the self-sustained oscillations is described by a reduced form of the classical van der Pol equation [8]. Encompassing the relevant parameters (nonlinear conductance of the electronic beam, ratio R/Q of the resonant cavity [13], DC beam resistance) of the dynamics of the RF field-electron beam interaction, an excitation equation is then obtained from which expressions for the starting current and saturation amplitude are readily derived [9, 10]**.** About the electrodynamic system, a coaxial Bragg reflector [6, 12] is connected on the back of the monotron to prevent radiation from leaking out of the wave guiding structure and also to electrically isolate the electron gun (held at a negative potential) from the body of the device, which is grounded. Including a coaxial guide periodically loaded by circular disks on the inner conductor, the reflector has been designed to operate at the 6.7 GHz frequency centered in a stop band as wide as possible. Experimental tests [7] have been performed on a stainless steel structure, from which the center frequency and a stop band 4.0-10.0 GHz wide have shown to be in good agreement with analytical and simulation results.

Plasma facing components

Materials facing the plasma in tokamak fusion reactors must withstand an enormous thermal load due to both radiation and particles emission from the plasma, while suffering minimum surface erosion by sputtering to avoid plasma contamination. A possible candidate to support these extreme conditions is diamond, due to singular properties as high hardness, low thermal expansion, high thermal conductivity, radiation resistance and chemical stability. Diamond coating of fusion plasma components can be obtained through the deposition of thin films, using the Hot Filament Chemical Vapor Deposition (HFCVD) method [24].

In order to verify the resistance of diamond films to plasma exposition, molybdenum samples coated with micro-crystalline CVD diamond films will be introduced in the ETE tokamak plasma edge. The results of this exposition will be analyzed in terms of the surface integrity of the samples, looking for damages in the diamond films by means of the Scanning Electron Microscopy (SEM) technique. Figure 28 shows the SEM image of a diamond film especially grown on a molybdenum substrate for insertion in ETE. This image shows the formation of a faceted micro-crystalline film. Characterization with Raman spectroscopy is also performed to verify the quality of the diamond films. On the right-hand side panel Fig. 28 shows the Raman spectrum of the diamond film shown on the left-hand side panel. The spectrum has a strong peak at 1332 cm^{-1}, which is characteristic of diamond. It also shows a broad peak between 1450 and 1650 cm^{-1}, which indicates the presence of graphite or amorphous carbon in the film. As the Raman spectroscopy is about 50 times more efficient for graphite than for diamond [26], this spectrum shows that the diamond film has a very good quality, with the deposition of much more diamond than graphite.

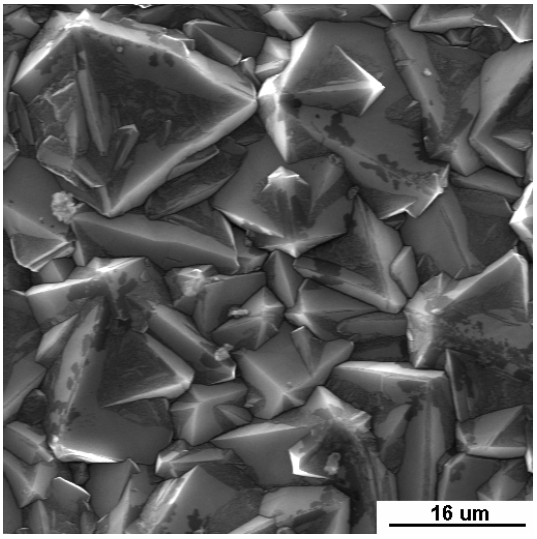

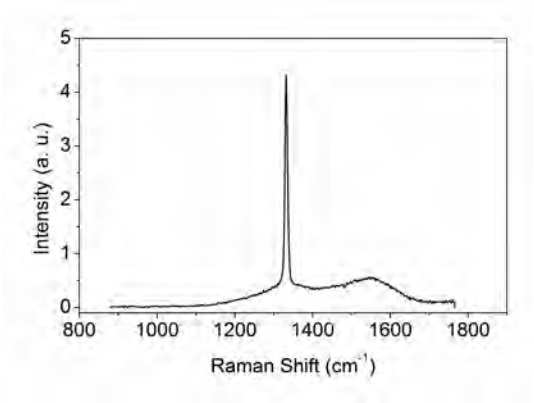

Fig. 28. Left: SEM image of the diamond film grown on molybdenum substrate. **Right:** Raman spectrum of the diamond film.

Vacuum conditioning

The hardware of the vacuum conditioning system of ETE as well as the vacuum system itself and the procedures adopted in the utilization of both systems have been continuously revised and improved over the last few years. Extra temperature monitors have bee added, shielding of thermocouple cabling has been improved to avoid spurious signals, etc. A systematic study has been carried out of the effects produced on impurity lines by both baking and glow discharge cleaning operations. Figure 29 shows a picture of the glow-discharge electrode in operation. Lately, the procedures for vacuum conditioning have been revised after a new set of graphite limiters and magnetic sensors was installed. As a result of that, an adequate conditioning routine was established for the present system. After a vacuum break, residual gas spectra without O_2 (partial pressure of line 32 below 10^{-8} Pa) and with partial pressure of line 18 (water vapor) below 2×10^{-6} Pa can now be obtained after about 60 h baking at 120 to 130°C as shown in the right-hand side panel of Fig. 29. After some additional baking the partial pressure of water vapor is reduced below 10^{-6} Pa, and further reduced by glow discharge cleaning. Replacing with copper gaskets the last few viton seals still employed in the system should allow in the near future baking operation at higher temperatures in order to completely remove water vapor from the inner walls of the ETE vacuum vessel.

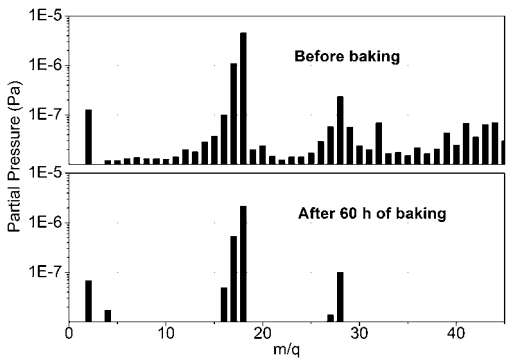

Fig. 29. Left: Picture showing the glow discharge electrode (bottom of the image) and the preionization filament. **Right:** Residual gas analysis just after a vacuum break (top) and after about 60 h of baking (bottom). The analysis after baking indicates removal of N_2 (m/q=28) and O_2 (32), traces of H_2 (2) and CO (28), but still considerable amounts of water.

Power systems and control

Design of a low cost double swing ohmic heating (OH) circuit using transformers as variable inductors controlled at the secondary, dissipating 10-15% of capacitor bank energy in the control resistor, has been carried out. Simulations shown in Fig. 30 indicate that pre-programmed control pulses with plasma current in the range 40 kA to 110 kA and corresponding pulse duration 30 ms to 15 ms can be achieved with the existent capacitor banks. Some switching components (IGBTs) have already been purchased for scaled-down tests of the concept. Detailed investigation of the toroidal field (TF) circuit has also been performed to identify and fix the causes of major and minor failures afflicting the present configuration. As a result, improvement in the TF circuit is being planned to reduce failure rate and to double the magnitude and duration of the magnetic field to 0.5 T, 20 ms. In addition, a new set of capacitor charging power supplies has been purchased to feed the flat-top sections of the TF capacitor bank, replacing the homemade chargers presently used with considerable improvement in charging time and reliability. Finally, following some improvements undertaken in the area of control and data acquisition, such as the purchasing and installation of a 64 channels data acquisition system, the implementation of automatic operation of the preionization filament, the development of a web interface for the ETE control software, etc., remote operation of ETE is now possible, not only from the ETE control room but from any computer terminal connected to the internet. Figure 30 also shows a picture of the initial 64 channels data acquisition system of ETE, which was recently upgraded to 256 channels

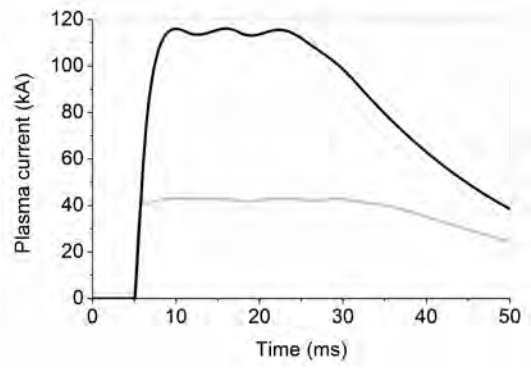

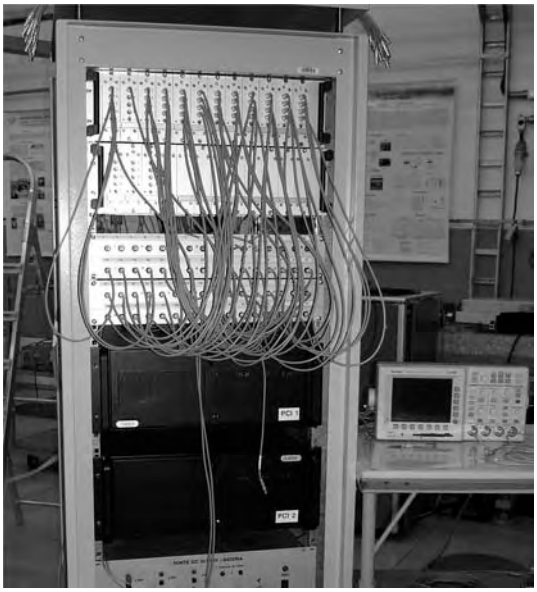

Fig. 30. Left: Simulation of the new OH power supply circuit showing plasma current pulses in the range from 40 to 110 kA. **Right:** 64 channels data acquisition system used for accessing the ETE diagnostics via web interface. This system was recently upgraded to 256 channels.

Acknowledgement The present work was partially supported by the International Atomic Energy Agency – IAEA (Research Contract No.: BRA/12932) and by the São Paulo Research Foundation – FAPESP.

References

1. **ANDRADE MCR, LUDWIG GO** (2005) Comparison of bootstrap current and plasma conductivity models applied in a self-consistent equilibrium calculation for tokamak plasmas, *Nuclear Fusion* **45**(1) 48-64
2. **ANDRADE MCR, LUDWIG GO** (2008) Scaling of bootstrap current on equilibrium and plasma profile parameters in tokamak plasmas, *Plasma Phys Control Fusion* **50**(4) 065001 (18pp)
3. **ANDRADE MCR, LUDWIG GO, DEL BOSCO E, NARAYANAN R, FERREIRA JG.** (2009) A fitting method for equilibrium reconstruction in ETE tokamak by using experimental magnetic signals, *10º Encontro Brasileiro de Física dos Plasmas – 10EBFP*, Maresias, SP, 22 a 25 de Novembro de 2009 (São Paulo: Sociedade Brasileira de Física, Program and Abstracts) p. 55
4. **BARROSO JJ** (2005) Stepped electric-field profiles in transit-time tubes, *IEEE Trans Electron Dev* **52**(5) 872-877
5. **BARROSO JJ** (2005) Optimizing the conversion efficiency of the monotron, *IMOC 2005* (Proc. IEEE/SBMO International Microwave and Optoelectronics Conference, Brasilia, Brazil, 25-28 July 2005) (Piscataway, NJ: IEEE, ISBN 0-7803-9342-2/05, December 2005) 133-136
6. **BARROSO JJ,** LEITE NETO JP (2006) Design of coaxial Bragg reflectors, *IEEE Trans Plasma Sci* **34**(3) 666-672
7. **BARROSO JJ, CASTRO PJ,** LEITE NETO JP, PIMENTEL GL (2007) Experimental characterization of a 6.7 GHz coaxial Bragg reflector, *Rev Sci Instrum* **78**, 096102(1-3)
8. **BARROSO JJ** (2007) Cavity excitation described by the van der Pol equation in transit-time tubes, *IEEE Trans Electron Dev* **54** (11) 3085-3091 DOI: 10.1109/TED.2007.907144
9. **BARROSO JJ** (2007) Onset and saturation of the electric-field amplitude in transit-time tubes, *Eighth IEEE International Vacuum Electronics Conference*, Kitakyushu, Japan, May 15-17, 2007 (Page(s):1-2, DOI 10.1109/IVELEC.2007.4283245)
10. **BARROSO JJ** (2007) Modeling transit-time microwave tubes, *IMOC 2007 International Microwave and Optoelectronics Conference*, October 29- November 1, Salvador, Brazil, 2007. Digest of Technical Papers, IEEE Catalog Number 07TH8919C, ISBN 1-4244-0661-7, pp. 297-301
11. **BARROSO JJ, ROSSI JO, CASTRO PJ,** GONÇALVES JAN, **DEL BOSCO E** (2007) Construction and tests of an injector electron gun for a 6.7 GHz monotron, *IMOC 2007 International Microwave and Optoelectronics Conference*, October 29-November 1, Salvador, Brazil, 2007. Digest of Technical Papers, IEEE Catalog Number 07TH8919C, ISBN 1-4244-0661-7, Library of Congress 2006933012, pp. 311-315
12. **BARROSO JJ, CASTRO PJ,** LEITE NETO JP, PIMENTEL GL (2008) Design and test of a 6.7 GHz coaxial Bragg reflector, *IEEE Trans Plasma Sci* **36**(2) part 2, 481-487 DOI: 10.1109/TPS.2008.917946
13. **BARROSO JJ,** LEITE NETO JP (2008) Resonance Frequency and Ohmic Q Factor in Klystron Cavities, *Ninth IEEE International Vacuum Electronics Conference*, April 22-24, 2008, Monterey, CA, USA. ISBN: 978-1-4244-1715-5, INSPEC Accession Number: 10072902, DOI 10.1109/IVELEC.2008.4556457, pp. 140-141
14. **BERNI LA,** ALONSO MP, **OLIVEIRA RM** (2004) Multipoint Thomson scattering diagnostic for the ETE tokamak, *Rev Sci Instrum* **75**(10) 3884-3886

15. **BERNI LA, DEL BOSCO E, OLIVEIRA RM,** ALONSO MP (2004) Thomson scattering diagnostic on the ETE tokamak: status and progress, *Braz J Phys* **34**(4B) 1572-1576
16. **BERNI LA,** ALBUQUERQUE BFC (2009) Stray light analysis for the Thomson scattering diagnostic of the ETE tokamak, *10º Encontro Brasileiro de Física dos Plasmas – 10EBFP*, Maresias, SP, 22 a 25 de Novembro de 2009 (São Paulo: Sociedade Brasileira de Física, Program and Abstracts) p. 38
17. **CASTRO PJ, BARROSO JJ** (2006) Radiation pattern measurements on a millimeter-wave open resonator, *Int J Infrared Millimeter Waves* **27**(10) 1323-1333
18. **CASTRO RM, NARAYANAN R, DEL BOSCO E, FERREIRA JG, LUDWIG GO, BERNI LA, ANDRADE MCR.** (2009) Estimation of ETE tokamak plasma column displacement using magnetic pickup coils, *10º Encontro Brasileiro de Física dos Plasmas – 10EBFP*, Maresias, SP, 22 a 25 de Novembro de 2009 (São Paulo: Sociedade Brasileira de Física, Program and Abstracts) p. 42
19. CODA S *et al* (2003) Electron cyclotron current drive and suprathermal electron dynamics in the TCV tokamak, *Nucl Fusion* **42** 1366-1370
20. **DEL BOSCO E, BERNI LA, FERREIRA JG, OLIVEIRA RM, LUDWIG GO, SHIBATA CS** (2005) Present Status of Operation of the ETE Spherical Tokamak, *Fusion Energy 2004* (Proc. 20th Int. Conf. Vilamoura, Portugal, 1-8 November 2004) (Vienna: IAEA, ISBN 92-0-100405-2, January 2005) CD-ROM file IC/P6-36, 7 pages and http://www-naweb.iaea.org/napc/physics/fec/fec2004/datasets/index.html
21. ESPOSITO B *et al* (1996) Runaway electron measurements in the JET tokamak, *Plasma Phys Control Fusion* **38** 2035-2049
22. ENTROP I (1999) Confinement of relativistic runaway electrons in tokamak plasmas, *Thesis work* submitted in December 1999 at Technische Universiteit Eindhoven, The Netherlands and http://alexandria.tue.nl/extra2/9903850.pdf
23. GALVÃO RMO, **LUDWIG GO, DEL BOSCO E, ANDRADE MCR,** LI J, WAN Y, WU Y, McNAMARA B, EDMONDS P, GRYAZNEVICH M, KHAIRUTDINOV R, LUKASH V, DANILOV A, DNESTROVSKIJ A (2008) Physics and engineering basis of multi-functional compact tokamak reactor concept, in *Fusion Energy 2008* (Proc. 22nd Int. Conf. Geneva, 2008)(Vienna: IAEA) CD-ROM file FT/P3-20 and http://www-naweb.iaea.org/napc/physics/FEC/FEC2008/html/index.htm
24. GOODWIN DG, BUTLER JE (1998) in PRELAS MA, POPOVICI G, BIGELOW LK (eds.) *Handbook of Industrial Diamonds and Diamond Films* (Marcel Dekker: New York 1998) pp. 527–581
25. HOANG GT *et al* (1997) *Proc. 24th EPS Conf.* (Berschtesgaden, Germany) vol 21A part III p. 965
26. KNIGHT DS, WHITE WB (1989) Characterization of diamond films by Raman-spectroscopy, *J Mater Res* **4**(2) 385-393
27. LÓPEZ-CALLEJAS R, BENÍTEZ-READ JS, LONGORIA-GÁNDARA LC, PACHECO-SOTELO J (2001) Plasma position measurement on the Novillo tokamak, *Fus Eng Design* **54**(1) 21-29
28. **LUDWIG GO, DEL BOSCO E, FERREIRA JG, BERNI LA, OLIVEIRA RM, ANDRADE MCR, SHIBATA CS, UEDA M, BARBOSA LFW, BARROSO JJ, CASTRO PJ, PATIRE Jr H** (2003) Spherical tokamak development in Brazil, *Braz J Phys* **33** (4) 848-859
29. **LUDWIG GO, FERREIRA JG, DEL BOSCO E** (2005) Eddy currents in the central column of the ETE spherical tokamak, *Fusion Eng Design* **73**(2-4) 343-356

30. **LUDWIG GO, DEL BOSCO E, FERREIRA JG** (2005) Eddy currents in the vacuum vessel of the ETE spherical tokamak, *Nucl Fusion* **45**(7) 675-684
31. **LUDWIG GO,** SABA MMF (2005) Bead lightning formation, *Phys Plasmas* **12**(9) 093509 (15pp)
32. **LUDWIG GO** (2006) The influence of edge viscosity on plasma instabilities, *Second IAEA Technical Meeting on the Theory of Plasma Instabilities: Transport, Stability and their Interaction*, Miramare, Trieste, Italy, 2-4 March 2005 (Vienna: IAEA, Proceedings Series, ISBN 92-0-102406-1, June 2006) File P-10, 8 pages and http://www-pub.iaea.org/MTCD/publications/PDF/P1255-cd/datasets/index.htm
33. **LUDWIG GO, FERREIRA JG, DEL BOSCO E, BERNI LA** (2006) Simulation of eddy currents in spherical tokamaks, *Nucl Fusion*, **46**(8) S629-S644
34. **LUDWIG GO** (2007) Relativistic distribution functions, fluid equations and equations of state for magnetized electron streams, *Plasma Phys Control Fusion* **49**(8) 1521-49
35. **LUDWIG GO** (2008) Macroscopic model of electron cyclotron current drive, *Plasma Phys Control Fusion* **50**(1) 025010 (19pp)
36. **LUDWIG GO, ANDRADE MCR,** GRYAZNEVICH M, TODD TN (2009) Physics performance analysis of low-power tokamak reactors, *Nuclear Fusion* **49**(8) 085026 (20pp)
37. **LUDWIG GO, ANDRADE MCR** (2009) Equilibrium evolution during tokamak startup, *10º Encontro Brasileiro de Física dos Plasmas – 10EBFP*, Maresias, SP, 22 a 25 de Novembro de 2009 (São Paulo: Sociedade Brasileira de Física, Program and Abstracts) p. 21
38. **LUDWIG GO, ANDRADE MCR,** GRYAZNEVICH M, TODD TN (2009) Low-power compact tokamak reactors, *10º Encontro Brasileiro de Física dos Plasmas – 10EBFP*, Maresias, SP, 22 a 25 de Novembro de 2009 (São Paulo: Sociedade Brasileira de Física, Program and Abstracts) p. 39
39. **NARAYANAN R, LUDWIG GO, FERREIRA JG, CASTRO RM, BERNI LA, DEL BOSCO E.** (2009) Experimental studies of energetic electrons in the ETE spherical tokamak using X-ray detectors, *10º Encontro Brasileiro de Física dos Plasmas – 10EBFP*, Maresias, SP, 22 a 25 de Novembro de 2009 (São Paulo: Sociedade Brasileira de Física, Program and Abstracts) p. 40
40. **OLIVEIRA RM,** UEDA M, **BERNI LA,** IGUCHI H (2004) Fast neutral lithium beam probing of the edge region of the spherical tokamak ETE, *Rev Sci Instrum* **75**(10) 3471-3474
41. **OLIVEIRA RM,** UEDA M, **BERNI LA** (2004) First results on the fast neutral lithium beam diagnostics probing the edge plasma of the ETE tokamak, *Braz J Phys* **34**(4B) 1655-1661
42. PETTY CC *et al* (2002) Detailed measurements of the electron cyclotron current drive efficiency on DIII-D, *Nucl Fusion* **42** 1366-1375
43. PEYSSON Y, IMBEAUX F (1999) Tomography of the fast electron bremsstrahlung emission during lower hybrid current drive on TORE SUPRA, *Rev Sci Instrum* **70**(10) 3987-4007
44. **ROSSI JO, BARROSO JJ,** RICOTTA DS, UEDA M (2005) A 30kV/24A hard-tube pulser for electron guns and microwave generators, *15th IEEE International Pulsed Power Conference*, Monterey, CA, USA, 13-17 June 2005, 4 pages
45. **ROSSI JO, BARROSO JJ,** UEDA M (2007) SPICE simulation for hard-tube modulator design, *16th International Pulsed Power Conference*, June 17-22, 2007, Albuquerque, NM, USA, 2007 IEEE Pulsed Power Conference Digest of Technical Papers ISBN 1-4244-0914-4, pp. 1305-1308
46. SHKAROFSKY IP (1982) Evaluation of multipole moments over the current density in a tokamak with magnetic probes, *Phys Fluids* **25**(1) 89-96

List of fusion related publications by members of the ETE spherical tokamak group and collaborators in the period 2005-2009

1. ALONSO MP, **BERNI LA,** VARANDAS CAF (2005) The fiber optic upgraded Thomson scattering diagnostic for the ISTTOK and the ETE tokamak, *Plasma Science Symposium 2005*, 22nd Symposium on Plasma Processing, Nagoya, Japan, 26-28 January 2005
2. ALONSO MP, **BERNI LA,** SEVERO JH, BORGES FO, ELIZONDO JI, MACHIDA M, VARANDAS CAF, GALVÃO RMO (2008) Multipoint Thomson scattering diagnostic for the TCABR tokamak with centimeter spatial resolution. In VARANDAS C, SILVA C (eds) *Plasma and Fusion Science* (Proceedings of the 17th IAEA Technical Meeting on Research Using Small Fusion Devices, Lisbon, Portugal, 22-24 October 2007) AIP Conference Proceedings **996**: 192-198 (ISBN-978-0-7354-0515-8, ISSN 0094-243X) and http://www.cfn.ist.utl.pt/17IAEATM_RUSFD/proceedings.html
3. ALONSO MP, FIGUEIREDO ACA, **BERNI LA,** VARANDAS CAF (2008) Simulation images of Doppler broadening for the Thomson scattering diagnostic of the TCABR tokamak, *IEEE Trans Plasma Sci* **36**, 1094-1095
4. ALONSO MP, FIGUEIREDO A, VARANDAS CAF, BORGES FO, LEONARDO J, ELIZONDO JI, SEVERO JH, NAJERA OU, GALVÃO RMO, **BERNI LA,** MACHIDA M (2009) Reconstruction activities and first results from the Thomson scattering diagnostic on the TCABR tokamak, *14th - International Symposium on Laser-Aided Plasma* Diagnostics, Castelbrando, Treviso, Italy, 21-24 September, 2009
5. **ANDRADE MCR, LUDWIG GO** (2005) Comparison of bootstrap current and plasma conductivity models applied in a self-consistent equilibrium calculation for tokamak plasmas, *Nuclear Fusion* **45**(1) 48-64
6. **ANDRADE MCR, LUDWIG GO** (2006) Scaling of bootstrap current in the framework of a self-consistent equilibrium calculation, *33rd EPS Conference on Plasma Physics* (Europhysics Conference Abstracts of the 33rd EPS Conference on Plasma Physics, Roma, Italy, June 19-23, 2006) Paper P1.189, 4 pages, http://crpppc42.epfl.ch/Roma/start.htm
7. **ANDRADE MCR, LUDWIG GO** (2008) Scaling of bootstrap current on equilibrium and plasma profile parameters in tokamak plasmas, *Plasma Phys Control Fusion* **50**(4) 065001 (18 pp)
8. **BARROSO JJ** (2005) Stepped electric-field profiles in transit-time tubes, *IEEE Trans Electron Dev* **52**(5) 872-877
9. **BARROSO JJ** (2005) Optimizing the conversion efficiency of the monotron, *IMOC 2005* (Proc. IEEE/SBMO International Microwave and Optoelectronics Conference, Brasilia, Brazil, 25-28 July 2005) (Piscataway, NJ: IEEE, ISBN 0-7803-9342-2/05, December 2005) pp. 133-136
10. **BARROSO JJ,** LEITE NETO JP (2005) Coaxial Bragg reflector, *IMOC 2005* (Proceedings IEEE/SBMO International Microwave and Optoelectronics Conference, Brasilia, Brazil, 25-28 July 2005) (Piscataway, NJ: IEEE, ISBN 0-7803-9342-2/05, December 2005) pp. 137-140
11. **BARROSO JJ,** LEITE NETO JP (2006) Design of coaxial Bragg reflectors, *IEEE Trans Plasma Sci* **34**(3) 666-672
12. **BARROSO JJ,** LEITE NETO JP (2006) A 6.6 GHz monotron with a coaxial Bragg reflector, *Seventh IEEE International Vacuum Electronics Conference*, Monterey, CA, USA, 25-27 April 2006, Conference Proceedings, pp. 325-326

13. **BARROSO JJ, CASTRO PJ,** LEITE NETO JP, PIMENTEL GL (2007) Experimental characterization of a 6.7 GHz coaxial Bragg reflector, *Rev Sci Instrum* **78**, 096102(3 pp)
14. **BARROSO JJ** (2007) Onset and saturation of the electric-field amplitude in transit-time tubes, *Eighth IEEE International Vacuum Electronics Conference*, Kitakyushu, Japan, May 15-17, 2007 (Page(s):1-2, DOI 10.1109/IVELEC.2007.4283245)
15. **BARROSO JJ** (2007) Start up and saturation in monotrons, *34th IEEE International Conference on Plasma* Science, Albuquerque, NM, USA, June 17-22, 2007. 2007 IEEE Pulsed Power Conference Digest of Technical Papers ISBN 1-4244-0914-4, pp. 1054-1057
16. **BARROSO JJ** (2007) Cavity excitation described by the van der Pol equation in transit-time tubes, *IEEE Trans Electron Dev* **54** (11) 3085-3091 DOI: 10.1109/TED.2007.907144
17. **BARROSO JJ,** LEITE NETO JP, **CASTRO PJ,** PIMENTEL GL (2007) Analysis and simulation of a 6.7 GHz coaxial Bragg reflector, *IMOC 2007 International Microwave and Optoelectronics Conference*, Salvador, Brazil, October 29-November 1, 2007. Digest of Technical Papers, IEEE Catalog Number 07TH8919C, ISBN 1-4244-0661-7, Library of Congress 2006933012, pp. 145-148
18. **BARROSO JJ** (2007) Modeling transit-time microwave tubes, *IMOC 2007 International Microwave and Optoelectronics Conference*, Salvador, Brazil, October 29- November 1, 2007. Digest of Technical Papers, IEEE Catalog Number 07TH8919C, ISBN 1-4244-0661-7, Library of Congress 2006933012, pp. 297-301
19. **BARROSO JJ, ROSSI JO, CASTRO PJ,** GONÇALVES JAN, **DEL BOSCO E** (2007) Construction and tests of an injector electron gun for a 6.7 GHz monotron, *IMOC 2007 International Microwave and Optoelectronics Conference*, Salvador, Brazil, October 29-November 1, 2007. Digest of Technical Papers, IEEE Catalog Number 07TH8919C, ISBN 1-4244-0661-7, Library of Congress 2006933012, pp. 311-315
20. **BARROSO JJ, CASTRO PJ,** LEITE NETO JP, PIMENTEL GL (2008) Design and test of a 6.7 GHz coaxial Bragg reflector, *IEEE Trans Plasma Sci* **36**(2) part 2, 481-487 DOI: 10.1109/TPS.2008.917946
21. **BARROSO JJ,** LEITE NETO JP (2008) Resonance Frequency and Ohmic Q Factor in Klystron Cavities, *Ninth IEEE International Vacuum Electronics Conference*, Monterey, CA, USA, April 22-24, 2008. ISBN: 978-1-4244-1715-5, INSPEC Accession Number: 10072902, DOI 10.1109/IVELEC.2008.4556457, pp. 140-141
22. **BARROSO JJ** (2009) Design study of a two-cavity monotron, *10th International Vacuum Electronics Conference-IVEC 2009*, Rome, Italy, 28-30 April, 2009 (Piscataway, NJ: IEEE Publishing, 2009) Book of Abstracts, v. 1, 2 pages, ISBN 978-1-4244-3499-2
23. **BARROSO JJ** (2009) Mechanism of efficiency enhancement in split-cavity electron-wave oscillators, *10th International Vacuum Electronics Conference-IVEC 2009*, Rome, Italy, 28-30 April, 2009 (Piscataway, NJ: IEEE Publishing, 2009) Book of Abstracts, v. 1, 2 pages, ISBN 978-1-4244-3499-2
24. **BARROSO JJ, CASTRO PJ, ROSSI JO,** GONÇALVES JAN (2009) Research and development in a high-power 6.7 GHz , *10th International Vacuum Electronics Conference-IVEC 2009*, Rome, Italy, 28-30 April, 2009 (Piscataway, NJ: IEEE Publishing, 2009) Book of Abstracts, v. 1, 2 pages, ISBN 978-1-4244-3499-2
25. **BARROSO JJ** (2009) Electron bunching in split-cavity monotrons, *IEEE Transactions Electron Devices* **56**(9) 2150-2154

26. **BARROSO JJ, CASTRO PJ,** LEITE NETO JP (2009) Experiments on Microwave Propagation through a Metallic Waveguide Loaded by an Array of Split-Ring Resonators, *IMOC 2009 – SBMO/IEEE MTT-S International Microwave and Optoelectronics Conference*, Belém, PA, Brazil, 03-06 November, 2009 (Proc. SBMO/IEEE, 2009, CD-ROM, p. 778-782) ISBN: 978-1-4244-5357-3
27. **BARROSO JJ** (2009) Conversion efficiency of transit-time microwave tubes, *IMOC 2009 – SBMO/IEEE MTT-S International Microwave and Optoelectronics Conference*, Belém, PA, Brazil, 03-06 November, 2009 (Proc. SBMO/IEEE, 2009, CD-ROM) ISBN: 978-1-4244-5357-3
28. **BARROSO JJ,** LEITE NETO JP (2009) Modeling and design of circular coupled cavities, *IMOC 2009 – SBMO/IEEE MTT-S International Microwave and Optoelectronics Conference*, Belém, PA, Brazil, 03-06 November, 2009 (Proc. SBMO/IEEE, 2009, CD-ROM) ISBN: 978-1-4244-5357-3
29. **BERNI LA, OLIVEIRA RM, DEL BOSCO E,** ALONSO MP (2006) 10-channel Thomson scattering diagnostic for the ETE tokamak, *16th Topical Conference on High-Temperature Plasma Diagnostic*, Williamsburg, VA, USA, 07-11 May 2006
30. **CASTRO PJ, BARROSO JJ** (2006) Radiation pattern measurements on a millimeter-wave open resonator, *Int J Infrared Millimeter Waves* **27**(10) 1323-1333
31. **CASTRO PJ, BARROSO JJ,** LEITE NETO JP, PIMENTEL GL (2007) Experimental tests on a coaxial Bragg reflector, *IMOC 2007 International Microwave and Optoelectronics Conference*, Salvador, Brazil, October 29-November 1, 2007. Digest of Technical Papers, IEEE Catalog Number 07TH8919C, ISBN 1-4244-0661-7, pp. 54-57
32. **CASTRO PJ, BARROSO JJ,** LEITE NETO JP (2008) Medição e cálculo do fator Q em cavidades ressonantes: discrepâncias e suas causa, *MOMAG 2008* (13º SBMO – Simpósio Brasileiro de Microondas e Optoeletrônica e 8º CBMag – Congresso Brasileiro de Eletromagnetismo), Florianópolis, SC, 7-10 de Setembro, 2008. *Anais*. Florianópolis: SBMag, 2008, CD-ROM pp. 1111-1115
33. **DEL BOSCO E, BERNI LA, FERREIRA JG, OLIVEIRA RM, LUDWIG GO, SHIBATA CS** (2005) Present Status of Operation of the ETE Spherical Tokamak, *Fusion Energy 2004* (Proc. 20th Int. Conf. Vilamoura, Portugal, 1-8 November 2004) (Vienna: IAEA, ISBN 92-0-100405-2, January 2005) CD-ROM file IC/P6-36, 7 pages and http://www-naweb.iaea.org/napc/physics/fec/fec2004/datasets/index.html
34. GALVÃO RMO, **LUDWIG GO, DEL BOSCO E, ANDRADE MCR,** LI J, WAN Y, WU Y, McNAMARA B, EDMONDS P, GRYAZNEVICH M, KHAIRUTDINOV R, LUKASH V, DANILOV A, DNESTROVSKIJ A (2008) Physics and engineering basis of multi-functional compact tokamak reactor concept, in *Fusion Energy 2008* (Proc. 22nd Int. Conf. Geneva, 2008)(Vienna: IAEA) CD-ROM file FT/P3-20 and http://www-naweb.iaea.org/napc/physics/FEC/FEC2008/html/index.htm
35. GRYAZNEVICH M, **DEL BOSCO E,** MALAQUIAS A, MANK G, VAN OOST G, **CRP Contributors** (2005) Joint research using small tokamaks, Fusion Energy *2004* (Proc. 20th Int. Conf. Vilamoura, 2004) (Vienna: IAEA) CD-ROM file OV/P6-15, 8 pages and http://www-naweb.iaea.org/napc/physics/fec/fec2004/datasets/index.html.
36. GRYAZNEVICH MP, **DEL BOSCO E,** MALAQUIAS A, MANK G, VAN OOST G, HE YEXI, HEGAZY H, HRON M, HIROSE A, KUTEEV B, **LUDWIG GO,** NASCIMENTO IC, SILVA C, VOROBYEV GM (2005) Joint research using small tokamaks, *Nucl Fusion* **45**(10) S245-S254

37. GRYAZNEVICH MP, **DEL BOSCO E,** MALAQUIAS A, MANK G, VAN OOST G, YEXI H, HEGAZY H, HRON M, HIROSE A, **LUDWIG GO,** KUTEEV B, NASCIMENTO IC, SILVA C, VOROBYEV GM (2006) Recent activities on the experimental research programme using small tokamaks, *16th IAEA Technical Meeting on Research Using Small Fusion Devices – RUSFD*, Ciudad del México, México, 30 November-2 December 2005 (AIP Conference Proceedings **875**: 120-128, 2006, ISBN 978-0-7354-8)
38. GRYAZNEVICH, MP, VAN OOST G, **DEL BOSCO E,** BERTA M, BROTANKOVA J, DEJARNAC R, DUFKOVA E, ĎURAN I, HRON M, ZAJAC J, MALAQUIAS A, MANK G, PELEMAN P, SENTKERESTIOVA J, STÖCKEL J, WEINZETTL V, ZOLETNIK S, TÁL B, **FERREIRA J**, FONSECA A, HEGAZY H, KUZNETSOV Y, RUCHKO L, VOROBJEV GM, OVSYANNIKOV A, SUKHOV E, SINGH A, KUTEEV B, MELNIKOV A, VERSHKOV V, KIRNEVA N, KIRNEV G, BUDAEV V, SOKOLOV M, TALEBITAHER A, KHORSHID P, GONZALES R, EL CHAMA NETO I, KRAEMER-FLECKEN AW, SOLDATOV V, FONSECA AMM, TAPIA CRG, KRUPNIK LI (2007) Progress on joint experiments on small tokamaks, *34th European Physical Society Conference on Plasma*, Warsaw, Poland, 2-6 July 2007
39. GRYAZNEVICH M, VAN OOST G, PELEMAN P, BROTANKOVA J, DEJARNAC R, DUFKOVA E, ĎURAN I, HRON M, SENTKERESTIOVA J, STÖCKEL J, WEINZETTL V, ZAJAC J, **BERNI LA, DEL BOSCO E, FERREIRA JG**, SIMÕES FJR, BERTA M, TÁL B, ZOLETNIK S, MALAQUIAS A, MANK G, FIGUEIREDO H, KUZNETSOV Y, RUCHKO L, HEGAZY H, OVSYANNIKOV A, SUKHOV E, VOROBJEV GM, DREVAL N, SINGH A, BUDAEV V, KIRNEV G, KIRNEVA N, KUTEEV B, MELNIKOV A, NUROV D, SOKOLOV M, VERSHKOV V, TALEBITAHER A, KHORSHID P, GONZALES R, EL CHAMA NETO I, KRAEMER-FLECKEN AW, SOLDATOV V, BROTAS B, CARVALHO P, COELHO R, DUARTE A, FERNANDES H, FIGUEIREDO J, FONSECA A, GOMES R, NEDZELSKI I, NETO A, RAMOS G, SANTOS J, SILVA C, VALCÁRCEL D, GUTIERREZ TAPIA CR, KRUPNIK LI, PETROV L, KOLOKOLTSOV M, HERRERA J, NIETO-PEREZ M, CZARNECKA A, BALAN P, SHARNIN A, PAVLOV V (2008) Results of joint experiments and other IAEA activities on research using small tokamaks, *Fusion Energy 2008* (Proc. 22nd Int. Conf. Geneva, Switzerland, 13-18 October 2008) Paper OV/P1-1
40. GRYAZNEVICH M, VAN OOST G, PELEMAN P, BROTANKOVA J, DEJARNAC R, DUFKOVA E, ĎURAN I, HRON M, SENTKERESTIOVA J, STÖCKEL J, WEINZETTL V, ZAJAC J, **BERNI LA, DEL BOSCO E, FERREIRA JG,** SIMÕES FJR, BERTA M, DUNAI D, TÁL B, ZOLETNIK S, MALAQUIAS A, MANK G, FIGUEIREDO H, KUZNETSOV Y, RUCHKO L, HEGAZY H, OVSYANNIKOV A, SUKHOV E, VOROBJEV GM, DREVAL N, SINGH A, BUDAEV V, KIRNEV G, KIRNEVA N, KUTEEV B, MELNIKOV A, NUROV D, SOKOLOV M, VERSHKOV V, TALEBITAHER A, KHORSHID P, GONZALES R, EL CHAMA NETO I, KRAEMER-FLECKEN AW, SOLDATOV V, BROTAS B, CARVALHO P, COELHO R, DUARTE A, FERNANDES H, FIGUEIREDO J, FONSECA A, GOMES R, NEDZELSKI I, NETO A, RAMOS G, SANTOS J, SILVA C, VALCÁRCEL D, GUTIERREZ TAPIA CR, KRUPNIK LI, PETROV L, KOLOKOLTSOV M, HERRERA J, NIETO-PEREZ M, CZARNECKA A, BALAN P, SHARNIN A, PAVLOV V (2009) Results of joint experiments and other IAEA activities on research using small tokamaks, *Nucl Fusion* **49**(10) 104026 (7 pp)

41. **LUDWIG GO, DEL BOSCO E, FERREIRA JG** (2005) Modeling and Measurement of Eddy Currents in the ETE Spherical Tokamak, *Fusion Energy 2004* (Proc. 20th Int. Conf. Vilamoura, Portugal, 1-8 November 2004) (Vienna: IAEA, ISBN 92-0-100405-2, January 2005) CD-ROM file TH/P4-7, 5 pages and http://www-naweb.iaea.org/napc/physics/fec/fec2004/datasets/index.html
42. **LUDWIG GO, FERREIRA JG, DEL BOSCO E** (2005) Eddy currents in the central column of the ETE spherical tokamak, *Fusion Eng Design* **73**(2-4) 343-356
43. **LUDWIG GO, DEL BOSCO E, FERREIRA JG** (2005) Eddy currents in the vacuum vessel of the ETE spherical tokamak, *Nucl Fusion* **45**(7) 675-684
44. **LUDWIG GO,** SABA MMF (2005) Bead lightning formation, *Phys Plasmas* **12**(9) 093509 (15 pp)
45. **LUDWIG GO, DEL BOSCO E, FERREIRA JG, BERNI LA** (2006) Determination of eddy currents in the vacuum vessel of spherical tokamaks, *Joint Meeting of the 3rd IAEA Technical Meeting on Spherical Tori and the 11th International Workshop on Spherical Torus*, St. Petersburg, Russia, 3-6 October 2005 (Vienna: IAEA, Working Material, 2006) CD-ROM file ETS-2, 9 pages and http://www.apmath.spbu.ru/iaea/
46. **LUDWIG GO** (2006) The influence of edge viscosity on plasma instabilities, *Second IAEA Technical Meeting on the Theory of Plasma Instabilities: Transport, Stability and their Interaction*, Miramare, Trieste, Italy, 2-4 March 2005 (Vienna: IAEA, Proceedings Series, ISBN 92-0-102406-1, June 2006) File P-10, 8 pages and http://www-pub.iaea.org/MTCD/publications/PDF/P1255-cd/datasets/index.htm
47. **LUDWIG GO, FERREIRA JG, DEL BOSCO E, BERNI LA** (2006) Simulation of eddy currents in spherical tokamaks, *Nucl Fusion*, **46**(8) S629-S644
48. **LUDWIG GO, DEL BOSCO E, BERNI LA, FERREIRA JG, OLIVEIRA RM, ANDRADE MCR, BARROSO JJ, CASTRO PJ, SHIBATA CS** (2006) Progress with the ETE experiment, *IAEA Second Research Co-ordination Meeting on Joint Research Using Small Tokamaks*, Beijing, China, 23-26 October, 2006 (Vienna: IAEA, document F1-RC-963.2, December 2006) pp. 51-60
49. **LUDWIG GO** (2007) Dynamics of electron cyclotron current drive, *Fusion Energy 2006* (Proc. 21st Int. Conf. Chengdu, China, 16-21 October 2006) (Vienna: IAEA, ISBN 92-0-100907-0 / ISSN 1991-2374, March 2007) paper TH/P6-12, 8 pages and http://www-naweb.iaea.org/napc/physics/FEC/FEC2006/html/index.htm
50. **LUDWIG GO** (2007) Relativistic distribution functions, fluid equations and equations of state for magnetized electron streams, *Plasma Phys Control Fusion* **49**(8) 1521-1549
51. **LUDWIG GO** (2008) Fluid model of electron cyclotron current drive. In VARANDAS C, SILVA C (eds.), *Plasma and Fusion Science* (Proceedings of the 17th IAEA Technical Meeting on Research Using Small Fusion Devices, Lisbon, Portugal, 22-24 October 2007). AIP Conference Proceedings **996**: 121-132 (ISBN-978-0-7354-0515-8, ISSN 0094-243X) and http://www.cfn.ist.utl.pt/17IAEATM_RUSFD/proceedings.html
52. **LUDWIG GO** (2008) Macroscopic model of electron cyclotron current drive, *Plasma Phys Control Fusion* **50**(1) 025010 (19pp)
53. **LUDWIG GO** (2008) Simplified design of a high temperature superconducting spherical tokamak, *First Meeting on the Use of HTS in Tokamaks*, Institute of Plasma Physics, Chinese Academy of Sciences, Hefei, Anhui, P.R. China, 20-22 February, 2008
54. **LUDWIG GO, ANDRADE MCR,** GRYAZNEVICH M, TODD TN (2008) Figure-of-merit Analysis of Low-power Spherical Tokamak Reactors, *4th IAEA*

Technical Meeting on Spherical Tori and *14th International Workshop on Spherical Torus*, Frascati, Rome, Italy, 7-10 October 2008 (Frascati, Italy: Italian Agency for New Technologies, Energy and the Environment – ENEA, Program) p. 27, Oral Communication

55. **LUDWIG GO, ANDRADE MCR,** GRYAZNEVICH M, TODD TN (2008) Performance analysis of low-power tokamak reactors, in *Fusion Energy 2008* (Proc. 22nd Int. Conf. Geneva, 2008)(Vienna: IAEA) CD-ROM file TH/P8-3 and http://www-naweb.iaea.org/napc/physics/FEC/FEC2008/html/index.htm
56. **LUDWIG GO, DEL BOSCO E, FERREIRA JG, ANDRADE MCR, BERNI LA, BARROSO JJ, CASTRO PJ** (2008) The ETE experiment and Brazilian plans for fusion, *IAEA Third Research Co-ordination Meeting on Joint Research Using Small Tokamaks*, Vienna, Austria, 20-24 October, 2008 (Vienna: IAEA, document F1-RC-963.3, November 2008) pp. 31-38
57. **LUDWIG GO, ANDRADE MCR,** GRYAZNEVICH M, TODD TN (2009) Physics performance analysis of low-power tokamak reactors, *Nucl Fusion* **49**(8) 085026 (20 pp)
58. **OLIVEIRA RM, BERNI LA,** UEDA M (2006) Improved Fast Neutral Lithium Beam Diagnostics for a Spherical Tokamak, *16th Topical Conference on High-Temperature Plasma Diagnostic*, 07-11 May 2006, Williamsburg, VA, USA
59. **ROSSI JO, BARROSO JJ,** RICOTTA DS, UEDA M (2005) A 30kV/24A hard-tube pulser for electron guns and microwave generators, *15th IEEE International Pulsed Power Conference*, Monterey, CA, USA, 13-17 June 2005, 4 pages
60. **ROSSI JO, BARROSO JJ,** UEDA M (2007) SPICE simulation for hard-tube modulator design, *16th International Pulsed Power Conference*, Albuquerque, NM, USA, June 17-22, 2007. 2007 IEEE Pulsed Power Conference Digest of Technical Papers ISBN 1-4244-0914-4, pp. 1305-1308
61. SANTOS AL, ARAÚJO FILHO BS, **BARROSO JJ,** MACIEL HS (2008) Microwave Generation by a Virtual Cathode Enclosed in a Circular Cavity Placed Transversally in a Cylindrical Waveguide, *Ninth IEEE International Vacuum Electronics Conference*, Monterey, CA, USA, April 22-24, 2008. ISBN: 978-1-4244-1715-5, INSPEC Accession Number: 10072979, DOI: 10.1109/IVELEC.2008.4556536, pp. 368-369
62. VAN OOST GEM, BERTA M, BROTANKOVA J, DEJARNAC R, **DEL BOSCO E,** DUFKOVA E, ĎURAN I, GRYAZNEVICH MP, HRON M, MALAQUIAS A, MANK G, PELEMAN P, SENTKERESTIOVA J, STÖCKEL J, WEINZETTL V, ZOLETNIK S, BALAZS T, **FERREIRA J,** FONSECA A, HEGAZY H, KUZNETSOV Y, OSSYANNIKOV A, SING A, SOKHOLOV M, TALEBITAHER A (2007) Joint experiments on small tokamaks, *Fusion Energy 2006* (Proc. 21st Int. Conf. Chengdu, China, 16-21 October 2006) (Vienna: IAEA, ISBN 92-0-100907-0 / ISSN 1991-2374, March 2007) paper EX/P4-34, 8 pages and http://www-naweb.iaea.org/napc/physics/FEC/FEC2006/html/index.htm
63. VAN OOST G, BERTA M, BROTANKOVA J, DEJARNAC R, **DEL BOSCO E,** DUFKOVA E, ĎURAN I, GRYAZNEVICH MP, HORACEK J, HRON M, MALAQUIAS A, MANK G, PELEMAN P, SENTKERESTIOVA J, STÖCKEL J, WEINZETTL V, ZOLETNIK S, TÁL B, **FERREIRA J,** FONSECA A, HEGAZY H, KUZNETSOV Y, OSSYANNIKOV A, SING A, SOKHOLOV M, TALEBITAHER A (2007) Joint experiments on small tokamaks: edge plasma studies on CASTOR, *Nucl Fusion* **47**(5) 378-386

8º Encontro Brasileiro de Física dos Plasmas – 8EBFP, Niterói, RJ, 27-30 de Novembro de 2005 (São Paulo: Sociedade Brasileira de Física, Program and Abstracts)

1. **ANDRADE MCR, LUDWIG GO.** Plasma profiles effects on the bootstrap current in a self-consistent equilibrium calculation, p. 20
2. **ANDRADE MCR, FERREIRA JG, LUDWIG GO.** Plasma resistance estimate in the ETE spherical tokamak by using a self-consistent equilibrium calculation, p. 21
3. **BARROSO JJ,** KOSTOV KG, UEDA M. Self-focusing and electron beam propagation in a plasma-filled gun, p. 18
4. **BARROSO JJ.** Electron beam interaction in coupled cavities of cylindrical symmetry, p. 18
5. **BARROSO JJ, CASTRO PJ, ROSSI JO,** GONÇALVES JAN, SANDONATO GM. Construction and test of a 5 A, 10 kV electron gun, p. 29
6. **BERNI LA, DEL BOSCO E, OLIVEIRA RM.** Design and preliminary results of a 10-channel Thomson scattering diagnostic for the ETE tokamak, p. 33
7. **DEL BOSCO E, LUDWIG GO, BERNI LA, FERREIRA JG, OLIVEIRA RM, SHIBATA CS.** Advances in the diagnostic system of the ETE spherical tokamak, Invited Talk, p. 11
8. LEITE NETO JP, **BARROSO JJ.** Tuning and electrical Q factor of reentrant cylindrical cavities, p. 19
9. **LUDWIG GO, DEL BOSCO E, FERREIRA JG, BERNI LA.** Electromotive force on the vacuum vessel wall of the ETE spherical tokamak, Oral Communication, p. 37
10. **OLIVEIRA RM,** UEDA M, **BERNI LA.** Fast neutral lithium beam probe system upgrade for plasma density profile measurements at ETE tokamak, p. 34
11. SANTOS AL, **BARROSO JJ,** ARAUJO FILHO BS. Exploring novel virtual cathode oscillator configurations, p. 23
12. **SHIBATA CS,** DE OLIVEIRA NG, **OLIVEIRA RM.** Data management and visualization in the ETE tokamak: current status and future directions, p. 35

9º Encontro Brasileiro de Física dos Plasmas – 9EBFP, São Pedro, SP, 25 a 28 de Novembro de 2007 (São Paulo: Sociedade Brasileira de Física, Program and Abstracts)

1. **ANDRADE MCR, LUDWIG GO.** Scaling of bootstrap current in tokamak plasmas, p. 33
2. **BARROSO JJ.** Excitation of circular electromagnetic cavities by a hollow electron beam, p. 47
3. **BARROSO JJ, ROSSI JO, CASTRO PJ,** GONÇALVES JAN, **DEL BOSCO E.** Construction and tests of an injection electron gun for producing a 20A/kV hollow beam, p. 46
4. **BERNI LA, DEL BOSCO E, LUDWIG GO, FERREIRA JG.** One-channel microwave interferometer for the ETE tokamak, p. 31
5. **BERNI LA, DEL BOSCO E,** ALONSO MP. 10-channel Thomson scattering diagnostic for the ETE tokamak, p. 31
6. **BERNI LA,** ALONSO MP, SEVERO JH, BORGES FO, ELIZONDO JI, MACHIDA M, VARANDAS C, GALVÃO RMO. Design of a multipoint Thomson scattering diagnostic for the TCABR tokamak, p. 31

7. **CASTRO PJ, BARROSO JJ**, LEITE NETO JP, PIMENTEL GL. Experiments on a coaxial Bragg reflector, p. 46
8. GRECO AFG, **DEL BOSCO E.** Electrostatic probe analyses for definition of procedures to automatically perform measurements of ETE edge plasmas, p. 37
9. LEITE NETO JP, **BARROSO JJ, CASTRO PJ**, PIMENTEL GL. Design and simulation of a 6.7 GHz coaxial Bragg reflector, p. 45
10. **LUDWIG GO.** Fluid model of electron cyclotron current drive, Oral Communication, p. 29
11. **LUDWIG GO,** NASCIMENTO IC, DILLENBURG D. Anteprojeto do Laboratório Nacional de Fusão – LNF, Comunicação Oral
12. ROUSSILLE AV, **DEL BOSCO E.** Magnetic probe system for equilibrium reconstruction of ETE tokamak plasmas, p. 37

10º Encontro Brasileiro de Física dos Plasmas – 10EBFP, Maresias, SP, 22 a 25 de Novembro de 2009 (São Paulo: Sociedade Brasileira de Física, Program and Abstracts)

1. **ANDRADE MCR, LUDWIG GO, DEL BOSCO E, NARAYANAN R, FERREIRA JG.** A fitting method for equilibrium reconstruction in ETE tokamak by using experimental magnetic signals, p. 55
2. **BARROSO JJ.** Enhancing conversion efficiency in microwave tubes, Oral Communication, p. 12
3. **BARROSO JJ,** LEITE NETO JP. Iris-coupled circular cavities for transit-time microwave tubes, p. 31
4. **BERNI LA,** ALBUQUERQUE BFC. Stray light analysis for the Thomson scattering diagnostic of the ETE tokamak, p. 38
5. BORGES F O, ELIZONDO R I, JERÔNIMO LC, NASCIMENTO IC, SANADA EK, SEVERO JHF, USURIAGA OC, GALVÃO RO, **BERNI LA,** MACHIDA M, ALONSO MP, VARANDAS CAF. Thomson scattering in TCABR: calibration and first measurements, p. 39
6. **CASTRO PJ, BARROSO JJ,** LEITE NETO JP. Experimental study on electromagnetic wave propagation through a metallic waveguide loaded by an array of split-ring resonators, p. 46
7. **CASTRO RM, NARAYANAN R, DEL BOSCO E, FERREIRA JG, LUDWIG GO, BERNI LA, ANDRADE MCR.** Estimation of ETE tokamak plasma column displacement using magnetic pickup coils, p. 42
8. **LUDWIG GO, ANDRADE, MCR.** Equilibrium evolution during tokamak startup, p. 21
9. **LUDWIG GO.** A figure-of-merit analysis of tokamak performance, p. 39
10. **LUDWIG GO, ANDRADE MCR,** GRYAZNEVICH M, TODD TN. Low-power compact tokamak reactors, p. 39
11. **NARAYANAN R, LUDWIG GO, FERREIRA JG, CASTRO RM, BERNI LA, DEL BOSCO E.** Experimental studies of energetic electrons in the ETE spherical tokamak using X-ray detectors, p. 40
12. **NARAYANAN R,** SEKAR IYENGAR AN. Investigation of runaway behaviour in the SINP tokamak, Oral Communication, p. 57